Order Number 8814256

Charge-coupled device optimizations for astronomy

Lesser, Michael Patrick, Ph.D.

The University of Arizona, 1988

U·M·I
300 N. Zeeb Rd.
Ann Arbor, MI 48106

PLEASE NOTE:

In all cases this material has been filmed in the best possible way from the available copy. Problems encountered with this document have been identified here with a check mark __✓__.

1. Glossy photographs or pages ✓
2. Colored illustrations, paper or print _____
3. Photographs with dark background ✓
4. Illustrations are poor copy _____
5. Pages with black marks, not original copy _____
6. Print shows through as there is text on both sides of page _____
7. Indistinct, broken or small print on several pages _____
8. Print exceeds margin requirements _____
9. Tightly bound copy with print lost in spine _____
10. Computer printout pages with indistinct print _____
11. Page(s) _____ lacking when material received, and not available from school or author.
12. Page(s) _____ seem to be missing in numbering only as text follows.
13. Two pages numbered _____. Text follows.
14. Curling and wrinkled pages _____
15. Dissertation contains pages with print at a slant, filmed as received _____
16. Other _____

_____

_____

CHARGE-COUPLED DEVICE OPTIMIZATIONS FOR ASTRONOMY

by

Michael Patrick Lesser

A Dissertation Submitted to the Faculty of the

DEPARTMENT OF ASTRONOMY

In Partial Fulfillment of the Requirements

For the Degree of

DOCTOR OF PHILOSOPHY

In the Graduate College

THE UNIVERSITY OF ARIZONA

1 9 8 8

THE UNIVERSITY OF ARIZONA
GRADUATE COLLEGE

As members of the Final Examination Committee, we certify that we have read the dissertation prepared by Michael Patrick Lesser

entitled Charge-coupled Device Optimizations for Astronomy

and recommend that it be accepted as fulfilling the dissertation requirement for the Degree of Doctor of Philosophy.

Edward Olszewski — 4/18/88
Edward Olszewski — Date

P. A. Strittmatter — 4/18/88
Peter Strittmatter — Date

Robert Leach — 4/18/88
Robert Leach — Date

William F. Hoffmann — 4/18/88
William Hoffmann — Date

J. Roger Angel — 4/18/88
J. Roger Angel — Date

Final approval and acceptance of this dissertation is contingent upon the candidate's submission of the final copy of the dissertation to the Graduate College.

I hereby certify that I have read this dissertation prepared under my direction and recommend that it be accepted as fulfilling the dissertation requirement.

J. Roger Angel — 4/18/88
Dissertation Director J. Roger Angel — Date

STATEMENT BY AUTHOR

This dissertation has been submitted in partial fulfillment of requirements for an advanced degree at The University of Arizona and is deposited in the University Library to be made available to borrowers under rules of the Library.

Brief quotations from this dissertation are allowable without special permission, provided that accurate acknowledgment of source is made. Requests for permission for extended quotation from or reproduction of this manuscript in whole or in part may be granted by the head of the major department or the Dean of the Graduate College when in his or her judgment the proposed use of the material is in the interests of scholarship. In all other instances, however, permission must be obtained from the author.

SIGNED: 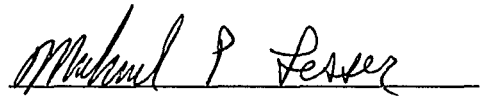

ACKNOWLEDGMENTS

It seems appropriate to first thank those who have contributed directly to this dissertation, my advisors Roger Angel and Bob Leach. Roger not only first thought that astronomers should sand their own CCDs, but has always inspired me with his continual stream of ideas. Bob has provided all of my formal CCD education, but perhaps more importantly, those daily philosophical discussions on just how it is that science gets done. I am especially grateful to Roger and Bob for their support considering the not-so-astronomical nature of this dissertation. Dr. Mirek Plavec at UCLA provided me with many opportunities for research and involvement in astronomy as an undergradute, which has certainly helped me throughout my graduate career. And my father, Robert Lesser, can take credit for getting me pointed in the right direction, and always providing the advice I needed along the way.

I think the best part of graduate school has been the enjoyable experience of knowing that there was nothing else I would rather be doing than what I actually had the chance to do. Of course I would rather have had more money to do it in a shorter time, but it has been fun and rewarding throughout. The reason for this is the people to which I have had the good fortune to be associated. Along with all the Steward faculty, staff, and graduate students I would like to especially thank Jill, Ted, Allen & Valerie, Kem & Jeannie, Steve, Mark, Walt, Richard, Chris, Connie, Charlie, Stacy, Bill & Cher, grumpy Bill, and EdO for their friendship. A special thanks has to go to Mike for adopting us and to John for being my pseudo-advisor and friend from my first year project to my dissertation defense. And of course, I could never exclude those two hounds who were always willing to wrestle with me no matter how late I came home, Barry and Gandy.

I also thank those who helped pay for my fun, including NASA grant NAGW-121, the U of A Graduate Student Program Development Fund, NSF SBIR grant ISI 87860599, and Steward Observatory.

Finally, and most importantly, I take a very special pleasure in thanking the two most important people in my life. First, my wife Doris, who has not only been my best friend for the past nine years but has made every moment worthwhile. Her love and encouragement is the primary reason I can write these acknowledgments today. And although he may not understand it now, my son Chris taught me on the day he was born that I never again had to worry about being a success.

TABLE OF CONTENTS

TABLE OF CONTENTS – continued

LIST OF ILLUSTRATIONS

LIST OF TABLES

Page

ABSTRACT

In the past decade, charge-coupled devices (CCDs) have rapidly become the astronomical imaging detector of choice for the visible and near-IR spectral regions. There are, however, several problems which have greatly reduced the availability of sufficient quality CCDs to the astronomical community. These include the low blue and ultraviolet quantum efficiency of thick devices, the lack of properly thinned devices, warped imaging surfaces, interference fringing, and the small size of the detectors themselves compared to telescope focal planes. This dissertation presents methods which can be used to optimize CCDs obtained from various manufacturers for astronomical observations. A new thinning technique which produces an optically flat surface across an entire CCD is demonstrated. A mounting technique which maintains a flat and stable imaging surface for thinned devices by bonding the CCD backside against a transparent glass support substrate is also demonstrated. Bump bonding of CCDs onto a silicon support before thinning is discussed as a future mounting/thinning technique. The design of antireflection coatings for the near-UV through near-IR spectral regions is explained and demonstrated on silicon diodes, allowing quantum efficiencies as high as 90% to be obtained. The reduction of interference fringing amplitudes by as much as 70% in the red and near-IR with AR coatings is also discussed. And finally, the design of CCD focal plane mosaics using the optimization techniques presented is discussed.

CHAPTER 1

CCDS IN ASTRONOMY

In recent years charge-coupled devices (CCDs) have become the astronomical detectors of choice for nearly all instruments requiring a two dimensional imaging sensor in the visible and near infrared spectral regions. This great popularity is due mainly to the CCD's high quantum efficiency, low noise, large dynamic range, and stable operating characteristics. These properties are greatly improved over previous generations of astronomical imaging devices such as image tubes and photographic plates. Considering the vast amount of observatory resources put into CCD detector programs worldwide, and anticipating the future trends of the semiconductor industry, it appears likely that CCDs will remain the dominate astronomical imagers in the visible and near IR for at least the next ten years. It is therefore advantagous for astronomers to fully optimize CCDs for their observational needs to obtain detectors of the highest possible quality and efficiency.

Great advances have been made by manufacturers in the last decade toward improving CCD characteristics, and much progress can be expected in the future. Current devices, however, have a number of characteristics that are far below their theoretical limits and have seen little recent improvement. Many of these are of prime importance to astronomers, such as absolute quantum efficiency, active imaging area, and flat field uniformity. The slow progress

in these areas can be attributed mainly to the technological difficulties of silicon processing. Quantum efficiency in the blue and UV is now limited by the solid state conditions at the silicon surface exposed to radiation. The maximum area of an integrated circuit is determined by production capabilities and the number of defects in a single silicon crystal. Flat field uniformity is determined by chip packaging techniques as well as silicon processing procedures such as mask alignment, oxide growth, metalizations, and in the case of back illuminated CCDs, thinning uniformity. The significant improvement of any of these characteristics requires extensive research and development expenditures. CCD manufacturers would realize little immediate economic gain because of the relatively few customers (such as astronomers) who would benefit from the improved devices. This dissertation describes techniques I have developed that can be applied to individual CCDs after their manufacture to obtain detectors of significantly higher quality than are currently available. The specific areas of detector optimization include thinning, antireflection coating, and backside charging for enhanced quantum efficiency, improved mounting for more uniform QE and image quality, and focal plane mosaic design for increased imaging area.

Current Optimization Procedures

Most CCD users have been able to optimize their detectors only by modifying those parameters that can be changed by controller electronics, such as gate voltages, waveform timing, and operating temperature. Many observatories have designed their own controllers to more fully optimize these parameters than is possible with commercial systems (*i.e.* Marcus *et al.* 1979,

Gunn *et al.* 1987, Robinson *et al.* 1987). As an example, most astronomical applications do not require rapid readout, therefore astronomers are willing to trade fast readout time for the lower noise that can be obtained with longer sampling times. A particular device is considered to be fully optimized when the best values of these "electronic" parameters have been found. But many important CCD characteristics are more difficult or impossible for astronomers to modify. These include pixel size, quantum efficiency and spectral response, detector area, cosmetic defects, and fringing amplitude. The only way to vary these characteristics has been to observe with different CCDs, which is always a tradeoff that introduces other undesirable characteristics. Furthermore, there are disappointingly few scientific grade CCDs available. Over the last decade, devices from only four manufactures have been used extensively for direct (unintensified) astronomical imaging or spectroscopy (Texas Instruments, RCA, GEC, and Thompson). This has limited the fundamental CCD characteristics which are available to astronomers. In contrast, as of early-1988, at least six scientific grade CCDs are known to be currently manufactured. In addition to these, there are now many smaller semiconductor foundries with the silicon processing capabilities for making scientific grade CCDs under contract. The means to convert readily available commercially produced CCDs into astronomical grade detectors is a primary goal of this disseration. This would greatly alleviate the unhealthy dependence modern astronomical instrumentation has placed on the success of a few commercial manufacturers. It is well known that astronomers have made great strides in the last century by adapting technologies developed for more lucrative markets (*e.g.* image tubes and photographic plates). The manufacture of solid state detectors is just such

a technology which can continue to be of great benefit to astronomy, especially if it is possible to modify the many commercially available sensors for use as astronomical detectors.

Optimizing Commercially Available CCDs

Table 1.1 and Figure 1.1 show a summary of some important characteristics of several scientific grade CCDs currently used for astronomical observations. The GEC, Thompson, and RCA devices are all built on commercial production lines intended mainly for manufacturing television grade devices. Scientific grade sensors are usually specially selected and tested for cold and low noise operation. The RCA CCD is thinned for improved blue and UV response, but is no longer available since RCA has stopped making CCDs. The Texas Instruments CCD is the only "astronomical" grade sensor, developed specifically for the Hubble Space Telescope Wide Field/Planetary Camera (Blouke *et al.* 1983) under contract with NASA. It is also thinned, but not commercially available. A limited number of TI sensors have been distributed to various observatories by the National Science Foundation, including three to Steward. They are excellent devices with high quantum efficiency when backside charged. The specific parameters quoted for the TI detector are those of our 90" telescope sensor after more than a man-year of optimization effort to achieve low noise and high UV response (Leach and Lesser 1987, Leach 1987).

It can be seen from Table 1.1 that most properties of the commercial scientific grade sensors are in no way inferior to those of the TI "astronomical" device. This is an important point when attempting to optimize commercial

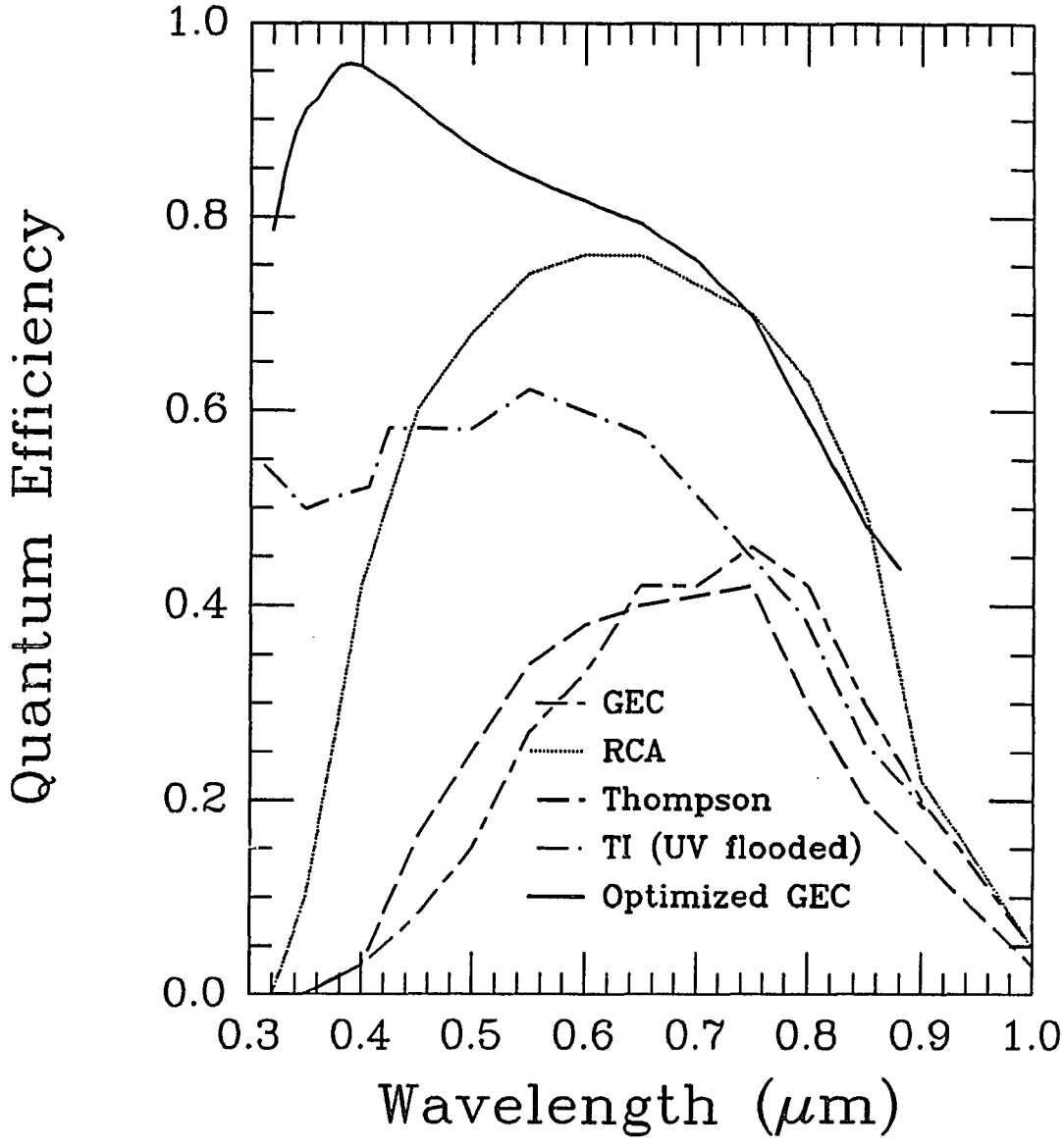

Figure 1.1. Quantum efficiency as a function of wavelength for the CCDs listed in Table 1.1 and as predicted for the GEC detector after thinning and optimization for maximum blue and UV response by the methods described in this dissertation. The thick GEC and Thompson data are from Thorne *et al* 1986. The TI data were measured after UV flooding with a cadmium lamp (Leach and Lesser 1987). The RCA data are from Leach 1987.

TABLE 1.1

Current Scientific Grade CCDs

Parameter	*GEC*[1]	*Thompson*[1]	*RCA*	*TI*
Device	P8603	TH7882	SID501EX	800x800 3ϕ
Format	385 x 578	384 x 576	320 x 512	800 x 800
Pixel size (μm)	22 x 22	23 x 23	30 x 30	15 x 15
Illumination	Front	Front	Back	Back
Noise (e^-)	5	5	37	6.2
Response uniformity				
pixel-to-pixel (%)	1.9	0.8	1.2	3.0
large scale blue (%)	7.6	2.4	2	30
large scale red (%)	2.4	0.4	20	20
Fringing?	No	No	Yes	Yes
Dark current				
(e^-/pixel/min at 150°K)	< 0.07	< 1.5	7[2]	< 0.06
Full well (e^-)	1.9 x 10^5	1.7 x 10^5	2.0 x 10^5	4.5 x 10^4

[1] From Thorne *et al.* 1986 [2] At 170°K for optimum CTE

CCDs for astronomical use because some parameters such as charge transfer efficiency, pixel-to-pixel uniformity, and minimum readout noise cannot be significantly altered after manufacture. Most other parameters, however, such as QE, large scale uniformity, and fringing are determined mainly by thinning and mounting techniques and can be greatly improved by the techniques presented in the following chapters. My QE goal for a CCD thinned to 15μm is shown as the uppermost curve of Figure 1.1. This is the calculated QE of CCDs such as

are currently in initial production at Ford, Reticon, Textronix, Thompson, and EEV after thinning, backside charging, and with the application of antireflection coatings. This particular curve shows a device optimized for blue and UV observations. Large scale response uniformity, fringing amplitude, and quantum efficiency can be significantly improved over what is currently obtained with a TI device. It can be clearly seen that commercial scientific grade CCDs, if fully optimized, have great potential for meeting the needs of the astronomical community and in fact becoming the finest detectors available to astronomers. What is lacking, and is the subject of this dissertation, is the ability to make the final optimizations of scientific grade CCDs to achieve the quantum efficiency, spectral response, and active area desired for astronomical observations. Although there has been some research from manufacturers and laboratories in recent years to obtain different devices with some of these characteristics, there has been no attempt to produce a single device with all of the properties desired for astronomical applications.

Quantum Efficiency Improvements

Some CCDs have measured quantum efficiencies in excess of 60% in the visible. Although this is extremely high compared to photographic plates (typically less than 4%) or image tubes (less than 20%), it is far from the theoretical performance of which a silicon detector is capable. There are several techniques that can be applied to CCDs after manufacture to increase QE to near its theoretical limit. These are briefly described below.

Thinning and Backside Charging

High quantum efficiency at wavelengths less than 4000Å has traditionally been very difficult to obtain with CCDs due to silicon's extremely high absorption coefficient in the blue and UV. CCDs are usually covered with polysilicon (silicon with only short range crystalline structure) on their frontside to make electrical connections to each pixel. This polysilicon is about 1μm thick and absorbs nearly all light below 4000Å. To avoid this loss some CCDs are operated in the back illuminated mode, where radiation is incident on the side opposite the electronic circuitry. This requires thinning the device to a thickness of less than $\approx 20\mu$m so that photo-generated electrons have a chance to diffuse through the silicon and reach the frontside potential wells. For these devices the blue and ultraviolet QE is determined by the solid state conditions at the back surface. Electrons photogenerated near this surface (predominately by short wavelength photons) are mostly trapped by a backside potential well, reducing the blue and UV quantum efficiency of the device considerably. In the last few years, however, a number of techniques have been developed to reduce this well and bring the QE of these sensors up to their reflection limited value. I describe in Chapter 2 a new method to thin CCDs for maximum blue and UV quantum efficiency, and in Chapter 4 discuss the backside treatment required to maintain this high QE. A new backside charging technique which allows permanent elimination of the backside potential well is presented.

Antireflection Coatings

Due to a back illuminated CCD's polished mirror-like surface, up to 60% of the radiation incident on the detector is lost by reflection. If appropriate antireflection (AR) coatings are applied directly to the CCD surface, this loss can be limited to less than 20% over the UV, visible, and near IR spectral regions. These coatings must be compatible with other methods of optimizing the detectors and should not degrade QE in any spectral region. Theoretical and experimental studies of AR coatings for astronomical CCDs have been completed and are disscussed in Chapter 3.

Thinned CCDs have suffered a problem in the red which has often given them a bad name – interference fringing due to multiple internal reflections off the silicon-air and silicon-silicon dioxide interfaces. This occurs because of silicon's high index of refraction but low absorption coefficient at longer wavelengths. Fringing can be reduced very effectively by the application of AR coatings on thinned devices. In addition, uniform thinning makes fringing more reproducible across the chip and therefore easier to remove with data reduction techniques. The effect of AR coatings on fringing is discussed in Chapter 3.

Device Uniformity Improvements

A major problem that affects accurate CCD observations is device nonuniformities. Pixel-to-pixel and large scale quantum efficiency variations make photometric calibrations very difficult. While little can be done by the astronomer to correct pixel-to-pixel variations other than careful calibration, a

number of techniques can be used to improve larger scale variations. These types of nonuniformities include fringing, defocus due to chip warping and movement, and thinning defects such as overly thin "hotspots" and large scale thickness variations. Some of these problems can be attributed directly to the technique used to mount the CCD in its carrier (defocus ripples and device movement). The remaining are due to thinning problems. Most pixel-to-pixel non-uniformity is due to variations in the frontside gate structure and actual pixel size, which can be changed only during manufacture. A mounting technique which improves device flatness to avoid defocus across the detector and is closely coupled to the new chem/mech thinning method is discussed in Chapter 2.

CCD Focal Plane Mosaics

A review of the literature from the semiconductor industry during the past decade shows that the average size of integrated circuits has consistently been decreasing. This is due to both the difficulty of producing large area devices free of defects and to the economic gain realized by producing many devices on a single wafer. Although large area CCDs have been anticipated for some time, they have yet to be delivered.

One possible method of obtaining a large detector area is to build a mosaic of many current-sized CCDs in the focal plane of the telescope. Although such a mosaic could find many uses even if it were not comprised of the best quality CCDs available, individual detectors in a mosiac should be as fully optimized as CCDs in single detector systems. This is necessary to justify

the high cost of a CCD mosaic since otherwise it would be more practical in many cases to take multiple exposures with a single fully optimized detector. As an example, if the detectors in a 2x2 mosaic achieved 20% QE at 4000Å (which is still better than the majority of CCDs today), a single CCD with 80% QE could cover the same area of sky in nearly the same time as the mosaic. If the image quality or quantum efficiency of a mosaic is poorer than that of a single detector, astronomers would probably prefer to take multiple exposures rather than use the mosaic. To fully justify the cost of a large area CCD mosaic the individual detectors must all be of the highest quality possible, and certainly no worse than the single detector systems available at the time. This design criterion has influenced the optimization techniques presented in the following chapters and constrained all research efforts to develop only those techniques that can be used with CCDs in a focal plane mosaic. The design of such a mosaic is discussed in Chapter 5.

Mosaic Controller Design Requirements

In order to realistically implement multi-chip detector systems such as focal plane mosaics, the controllers used to operate the individual detectors must be much more sophisticated than those now used. Many functions that are routinely done manually should be automated due to the sheer manpower required to maintain all the detectors at their optimum performance level. As an example, the initial start-up of a single present day CCD may take many weeks to fully optimize all the electronic parameters that control the chip (voltage levels, pulse widths and shapes, video processing parameters, temperature, etc.). A large mosaic of ten or more detectors would make this time scale

impractical from an operational standpoint. Shortcuts must be implemented to allow devices to be optimized through sophisticated computer control and image processing.

Along the same lines the data acquistion system must be changed in order to spend as much time actually observing each night as possible. If a single CCD takes 30 seconds to read out its image, a 10 chip mosaic would require 5 minutes to read out in series. This is not very practical, so parallel processing is necessary. Computers must be used that can receive data from many detectors simultaneously and efficiently store the images. The basic image processing functions such as bias subtraction and flat field calibration must be done on-line at the telescope to reduce the tremendous data storage and analysis problem a mosaic would create. These controller design considerations are discussed in Chapter 5.

Applications to Other Detectors

Because CCDs are silicon devices, any optimization techniques developed that relate directly to the silicon material can in principle be applied to other types of silicon photodetectors. As an example, silicon photodiodes have characteristics that make them more suitable than CCDs for certain projects, mainly due to their low cost, high speed, and large area. Advances are continuously being made in photodiode technology, especially with amorphous semiconductors, due to the world-wide interest in solar power conversion. The key to successful astronomical instrumentation is often the ability to use devices developed for other applications for astronomically important problems.

A field which has grown rapidly in recent years is infrared detector development. Silicon devices cannot detect light of wavelength longer than about 1.05μm due to silicon's bandgap of 1.1 eV. For IR observations, detectors of germanium, indium-antimony, mercury-tellurium, or other semiconductors must be used. The technology of processing these materials and building devices from them is immature compared to silicon technology, and a great deal of solid state physics is still to be learned concerning the interface, bulk, surface, and noise properties of such materials. Much of what is learned from improving the characteristics of silicon devices may be applicable in some way to improving IR detectors. Techniques to be discussed in this dissertation such as thinning, mounting, and antireflection coatings are directly applicable to solid state imagers of any type, while other QE enhancement techniques such as backside surface charging may apply to silicon devices only. Future experimentation and better theoretical understanding is required to know with certainty what techniques can cross over to the IR detector world.

Although silicon CCDs can be used as far UV and x-ray detectors (*i.e.* Luppino *et al.* 1987, Stern *et al.* 1987, Griffiths *et al.* 1981), the optimization procedures developed in this dissertation are intended for the spectral region from the atmospheric cutoff at 3100Å to the silicon response limit at 1.05μm. Many of these techniques, however, are directly applicable to shorter wavelength detectors. The differences between AR coatings used in the visible and those required for much shorter wavelengths (as might be appropriate for space missions) will be discussed. Thinning and mounting techniques are appropriate for all wavelength regions, although the desired device thickness depends on silicon properties in the wavelength region of interest. Backside charging is

also required for good far UV and x-ray performance. It is interesting to realize that deep depletion CCDs that have been built for x-ray observations have excellent potential as imagers in the red and near IR spectral regions. By careful characterization and understanding of CCDs designed for many different applications, and with the development of techniques such as those presented here, it is possible to modify current generation CCDs to obtain nearly ideal detectors for most astronomical needs for which silicon is a viable sensor.

CHAPTER 2

CCD THINNING AND MOUNTING

Two of the most important characteristics of astronomical detectors are broadband sensitivity and spatial and temporal stability. Optimized CCDs should therefore have high quantum efficiency from the atmospheric cutoff at 3100Å to the silicon response limit near 1μm with minimal spatial variation. For calibration purposes, QE variations with wavelength should also be small so that color differences between program objects and calibration sources do not introduce significant errors. The influence that the thinning and mounting of CCDs has on their spectral response, uniformity, and stability is discussed in this chapter. I describe a new thinning technique which allows very precise thickness control and can be used on nearly all CCDs. A mounting/packaging technique for thinned CCDs which maintains a flat surface to avoid the defocus problems associated with surface ripple is also discused.

CCD Spectral Response

Radiation incident on CCDs operated in the front illuminated mode must pass through the frontside gate structure before being detected. This gate structure is composed of an electrical conductor (either aluminum or more commonly polysilicon) and various oxide/nitride insulator levels. Polysilicon,

which has optical properties similiar to crystalline silicon, absorbs almost all light below 4000Å. Front illuminated CCDs therefore have little or no blue and UV spectral response. It is for this reason that CCDs are often operated in the back illuminated mode in which radiation is directly incident on the silicon lattice. Figure 2.1 shows a schematic representation of a typical CCD (here an EEV P86000) for reference purposes.

Silicon is capable of detecting radiation of all wavelengths shorter than its energy bandgap edge near 1.05μm. However, throughout this broad spectral range its absorption properties vary tremendously. The absorption length (distance over which a fraction $1/e$ of photons are absorbed) is 80μm at $\lambda = 1\mu$m and 40Å at 0.29μm. When optimizing devices for the ground-based astronomical region, it is desirable to have very thick CCDs for observations redward of about 7000Å and very thin devices toward the blue. Unfortunately, most observatories are unable to either obtain or maintain separate astronomical grade CCDs for these regions. Furthermore, all scientific grade CCDs currently manufactured are built on epitaxial layers less than 25μm thick. Electrons photogenerated outside this epitaxial region have a very small chance of being detected due to their short diffusion length in the substrate material. And since the depletion depth of such devices extends less than 10μm from the frontside, photoelectrons generated in the "field-free" region between the back surface and the back edge of the depletion region often diffuse to adjacent pixels for collection, reducing spatial resolution and effective quantum efficiency. The most sensitive CCD is therefore a thinned back illuminated device with an electric field at its back surface to force electrons directly to the frontside collection wells. This electric field can either be generated from the frontside

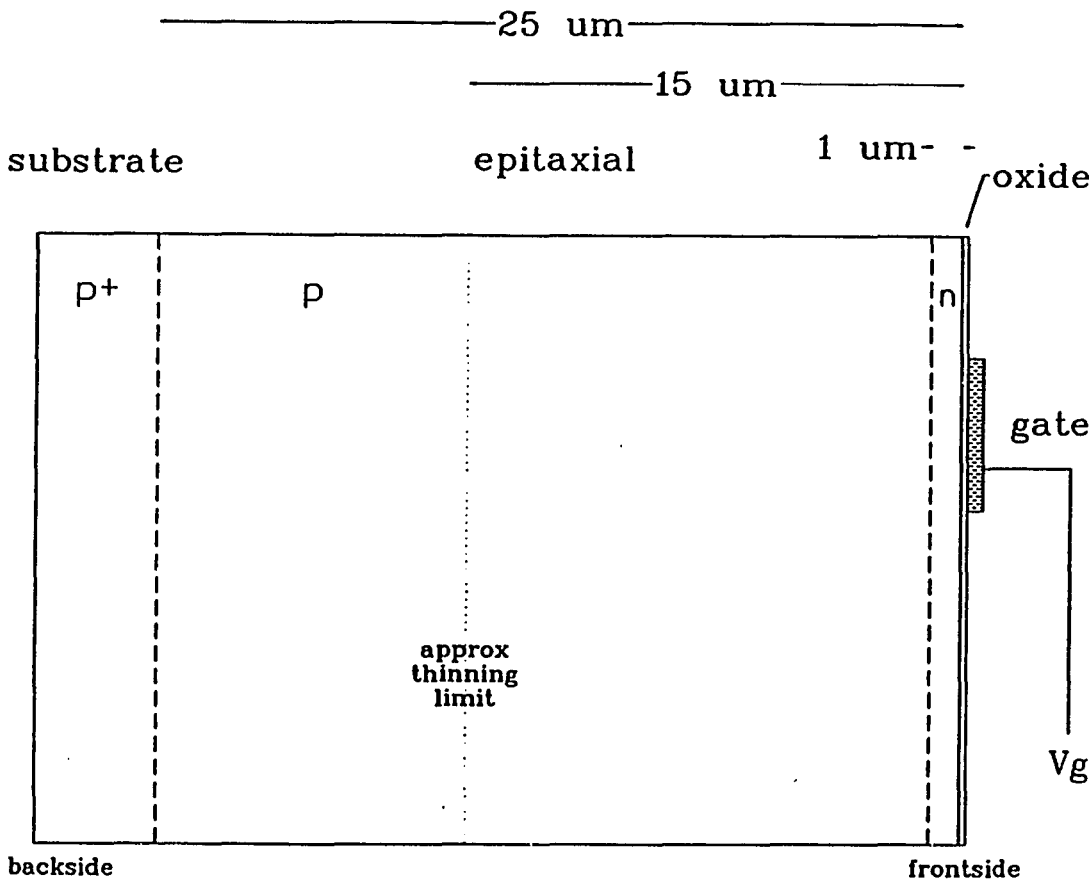

Figure 2.1. A schematic representation of the internal silicon structure of a EEV P86115 CCD. The epitaxial p-silicon layer is grown on the more heavily doped p^+-silicon substrate. For back illuminated operation the device should be thinned to about 15μm from an initial thickness of 600μm. One gate of a three gate pixel is shown on the frontside.

gate potentials (the depletion well), or induced from backside charging. Figure 2.2 shows the QE of such a CCD as a function of thickness for several wavelengths in the red and near IR. It can be seen that a thickness of at least 10μm is necessary for maximum QE in the visible and red, where most astronomical CCD observations are made.

While thinning CCDs for back illuminated operation has proven very successful for two scientific CCD manufacturers (Texas Instruments and RCA), there is another means of boosting blue and UV quantum efficiency. Thin films of organic UV downconverting phosphors have been applied to the frontsides of many devices. Considerably success has been reported by astronomers using coated GEC and Thompson devices (Cullum *et al.* 1985, Béal *et al.* 1987). The Wide Field/Planetary Camera for the Hubble Space Telescope was designed for TI 800x800 CCDs using a coronene film on the back surface (Blouke *et al.* 1983, Blouke *et al.* 1980). These dyes absorb UV photons and re-emit by fluorescence at longer wavelengths to which the CCD is more sensitive (around 6000Å). Although this is a much simpler and inexpensive way to gain blue and UV response, the highest QEs reported so far are about 20%, and the films are not very durable. I have therefore chosen to develop a means of thinning CCDs after manufacture with the uniformity and thickness control required to obtain high quality back illuminated detectors.

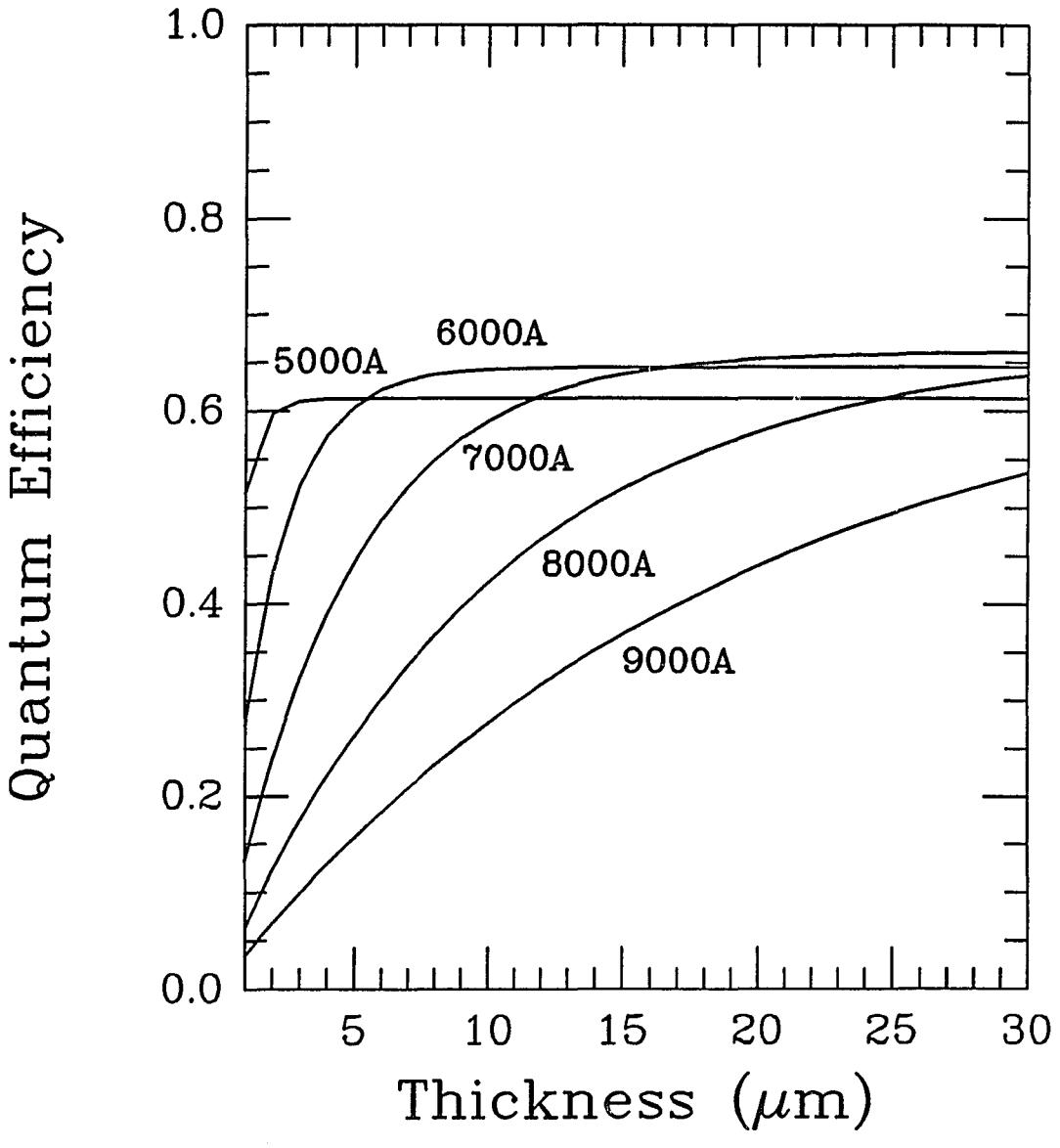

Figure 2.2. A comparison of the predicted quantum efficiency of a back illuminated CCD at several wavelengths as a function of device thickness. It is assumed that full backside charging is achieved, and there is no influence from residual backside p^+ material. The epitaxial thickness must therefore be several microns thicker than the thinnest point. The different maximum QE values are due to reflection differences at the various wavelengths.

Thinning Requirements

Many cosmetic defects such as pits, hills, and rings have been found in previous generations of thinned CCDs which contribute to non-uniform QE. These local thinning variations affect red and blue sensitivity in different ways. Red QE is directly proportional to the device thickness, as shown in Figure 2.2. From the slope of the lines in this figure it can be seen that thicker devices have much smaller QE variations resulting from thickness variations introduced during thinning. A thickness variation of only 1μm causes a QE change of several percent in the near IR if the device is thinner than 10μm. It is therefore necessary to achieve very precise and uniform thinning, and to use CCDs capable of operating when thicker than 10μm. This requires devices built on epitaxial layers $\approx 20\mu$m thick. Blue QE is extremely sensitive to the solid state conditions at the back surface because of silion's short absorption depth in this spectral region. If thickness variations extend through regions of different doping concentrations (as in the region surrounding the epitaxial-substrate interface), the effect of the backside charging used to eliminate the backside potential will also be variable. Blue and UV QE will therefore also vary as a function of device thickness (see Chapter 4). Current generation devices are in fact very sensitive to local thinning variations. For this reason CCDs must be thinned through the epitaxial diffusion region, which extends approximately 2μm inside the epitaxial-substrate interface on most CCDs. For the TI 800x800 devices this requires a total thickness of less than 8μm. Other CCDs with thicker epitaxial layers can be thinned to about 15μm (EEV, Ford, Reticon).

My initial thinning goal was to produce a surface quality superior to that of the Texas Instruments 800x800 3-phase CCDs developed for the HST Wide Field/Planetary Camera. My reasoning has been that these devices are of exceptional quality in terms of their electronic properties but suffer considerably from nonuniformities caused by acid thinning. Steward Observatory operates several of these sensors with excellent results. Their major drawback is local sensitivity variations of 20 to 30 percent (and its rippled surface, which will be discussed in a later section). After extensive extensive experimentation with acid thinning, I found that the surface quality desired for astronomical CCDs is extremely difficult to achieve. Thinning uniformity is critically dependent on agitation techniques, required to keep the acid flowing evenly across the silicon surface. It became apparent that thinning only the central region of the CCD was largely responsible for uneven thinning rates, due to acid "pooling" and uneven acid flow. Masking the edges of single devices is required, however, to avoid etching the edges of the device and ruining the circuitry. When I duplicated the exact thinning technique used by TI for the 800x800 CCDs (Janesick, 1987) I found the method to be dependent on the silicon epitaxial–substrate structure of the TI device. It does not work for thinning bulk silicon and must be modified for other epitaxial structures. For example, the EEV devices purchased have 25μm thick epitaxial layers but should be thinned to about 15μm for good QE and spatial resolution. Acid solutions can be devised which stop at the epitaxial interface and new solutions used to very slowly thin further. However, as the device is thinned inside the epitaxial interface the surface becomes less and less uniform due to thinning rate variations caused by local temperature, agitation, and chemical concentration fluctuations.

These factors are nearly impossible to control over the entire surface of a CCD to the precision required for the highest quality astronomical detectors. For these reasons I have developed a chemical/mechanical thinning technique which produces an optically flat surface and can be directly applied to a wide variety of devices. The final thickness does not depend on the epitaxial thickness of the device as with acid thinning techniques. Although mechanical action is used to maintain surface quality, the final silicon removal is chemical to eliminate any subsurface damage which would cause excessive recombination and dark current. This thinning method and results of laboratory experiments using setup grade CCDs are described in the following sections.

Chemical/Mechanical Thinning

The chem/mech thinning method proceeds in two distinct steps – initial loose abrasive lapping and final chem/mech polishing. CCDs are typically 500 – 600μm thick when received from the manufacturer. They must be thinned to 15μm or less for most existing CCDs structures, as discussed above. Because my final polishing method removes silicon at the rate of less than 1μm/min, abrasive lapping is necessary to initially thin the CCD to approximately 100μm. Lapping allows precise corrections for tilts introduced during thinning while the final chem/mech polishing does not. Lapping silicon is straightforward and quite similar to producing glass optical flats. The CCD is waxed with its frontside against a glass support (of matching expansion coefficient). It is surrounded by several silicon samples ("outriggers") which are used to keep the support from tilting. By monitoring the thickness of each outrigger during the

thinning process (with a dial indicator) it is possible to detect any tilts being introduced before they significantly affect the CCD. These tilts are corrected simply by shifting weight to the periphery of the glass disk for a short time, increasing the thinning rate where needed. The wax used to secure the silicon is several microns thick and must be applied with great care to maintain the necessary uniformity. Nearly all bow (uniform thickness variation from the center outward) or tilt in a chem/mech thinned device can be attributed to nonuniform mounting wax. The actual lapping takes place against the cast iron plate of a Lapmaster 12 lapping machine, shown in Figure 2.3. Aluminum oxide slurry is used in two stages, with 12 and 3 micron particles, respectively. The thickness limit of the abrasive process was determined to reduce the polishing time required and to ensure that all the mechanically damaged silicon is removed in the polishing operation. The 12μm lapping stage stops at a thickness of 200μm and the 3μm stage at 100μm. Subsurface damage extends inward about five times the slurry particle size, or to about 80μm from the frontside when lapping is completed. Polishing to 15μm entirely removes any damaged silicon. This has been verified by acid etch studies of the chem/mech polished surface.

After the CCD is mechanically lapped the polishing begins. I have adapted a chemical/mechanical process originally developed at IBM for the polishing of silicon wafers before epitaxial growth (Regh and Silvey 1968). From published accounts, it seems this method was used only a short time for silicon polishing, and never for other applications such as thinning. In this cupric ion process, a layer of copper is plated on the CCD backside which reacts with the silicon by oxidization. The copper and oxidized silicon are then

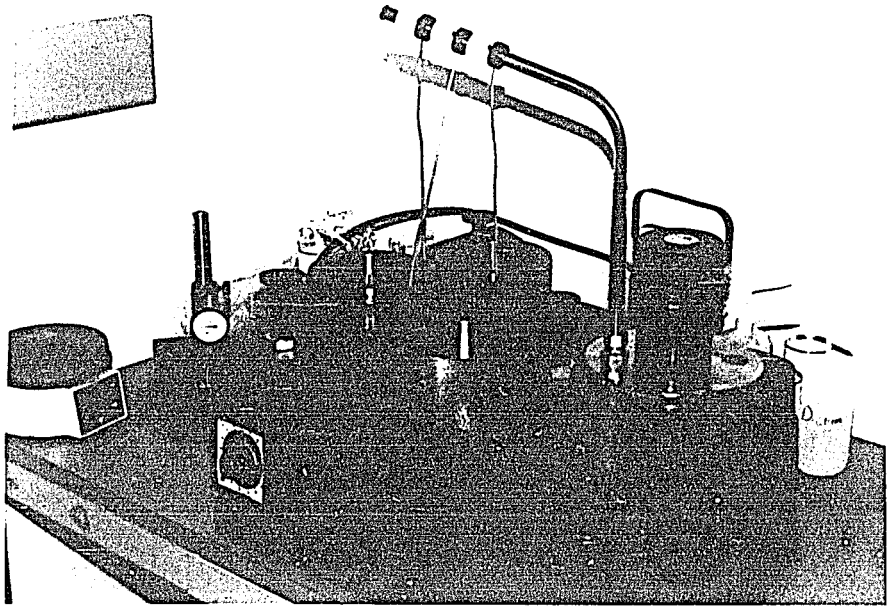

Figure 2.3. The Lapmaster 12 lapping machine used for the chemical/mechanical thinning of CCDs. The glass thinning support disk is placed in one conditioning ring with weights on top. The other rings are used to keep the lapping plate (cast iron) true. For polishing the plate is covered with a soft polishing matrix such as a PELLON pad.

mechanically removed by the wiping action of a soft polishing matrix (Pellon pad or Microcloth). The silicon removal process takes place in several steps as follows (Mendel and Yang 1969).

$$Cu^{+2} + 2e^{-} \longrightarrow Cu^{0}$$

$$Si^{0} \longrightarrow Si^{+4} + 4e^{-}$$

$$Si^{+4} + 6F^{-} \longrightarrow SiF_6^{-2}$$

$$SiF_6^{-2} + 2(NH_4)^{+} \longrightarrow (NH_4)_2SiF_6.$$

The Cu^{+2}, F^{-}, and $(NH_4)^{+}$ are provided by the ionic polishing solution, the Si^{0} is the CCD backside surface, and the Cu^{0} is wiped from that surface by the polishing cloth to enable the reactions to continue indefinitely. Since the silicon interaction is essentially chemical, there is no subsurface damage. Furthermore, since the removal rate is determined by mechanical action, all the control of true optical polishing is obtained. Surface flatness of less than one micron is easily obtained as verified by interference against an optical flat. The major difficulty with this thinning technique is due to the fragility of the entirely thinned silicon. Problems include the chipping of the CCD's edges during polishing and removing the delicate thinned device from the thinning support. This has been the main failure mode, with the present yield being about 75%. A detailed recipe of the thinning process is included in Appendix A.

Chem/Mech Thinning Results

The quality of the resultant surface is dependent on factors such as solution composition, lap speed, applied pressure, mounting technique, polishing cloth type, and the method of process termination. While all of these can be precisely controlled during the thinning operation, the determination of the proper conditions for successful thinning is quite difficult. The development of the process to the point where 15μm devices can be routinely obtained with reasonable yield has taken several years. It has been found that there is no substitute for Pellon polishing cloth, even though many other softer cloths were tried in hopes of reducing edge chipping. Softer cloths with higher pile are unable to wipe the plated copper off the CCD, in which case the chemical thinning process stops. Thinning no longer continues evenly and a very rough surface is obtained. I have found that the uniform removal of the plated copper is the most important factor influencing the surface quailty. Uniform copper removal is also determined by the applied pressure of the CCD on the polishing cloth. A great improvement in surface quality was obtained when the CCDs and outriggers were waxed to microscope slide glass plates which were in turn waxed to the larger glass disk (4" diameter). This allows only a small area of glass in three distinct areas to contact the polishing cloth, and much better control of surface pressure is obtained. It was also found that some CCDs, all from one manufacturer, could only be thinned when polished to a specular surface before beginning the final chem/mech step. Other CCDs could be chem/mech thinned directly after the lapping stage. The reason for this is unclear. The method used for termination of each thinning cycle (about

20 minutes) is also important for obtaining a high quality surface. By flooding the polishing cloth for at least one minute before stopping the cloth rotation, all copper is uniformly removed for the CCD and the next step will procede uniformly. If copper is left on the device between cycles, uneven polishing may occur. It has been reported by the original IBM research that some silicon resistivities (high doping concentrations) do not polish well using this method, although my experiments have demonstrated that the method works well on the types of silicon used for CCD fabrication. The only poor results have been encountered with very highly doped silicon. Since future CCDs will most likely use silicon with lower doping concentrations for deep depletion and easier backside charging, I expect this process to remain an ideal thinning technique for many years. Thin sample devices flat to $\pm 0.5\mu$m across the entire device are now routinely produced. These experiments have been done with bulk silicon and 20 and 25μm epitaxial layer silicon, typically thinned to 15μm. Thickness measurements are made with a dial indicator referenced to the original thickness of the device. The thickness measurements of a thinned device have been confirmed by interference fringe counting using a scanning infra-red spectrophotometer. The color of light transmitted through the CCD (thinned to less than about 20μm) is also indicative of the thickness. Attempts to thin to less than 15μm have proven unsuccessful with the chem/mech process due to excessive edge chipping. I believe this is near the limit of the technique, and thinner devices might be better produced using other methods. This limit is responsible for the low yield of my early work when I attempted to make all devices thinner. The 15μm thickness limit is no limitation for CCDs built on epitaxial layers which are 20μm or thicker. Fortunately, most CCDs currently

being produced have such epilayers and can be chem/mech thinned. Older devices such as the TI 800x800 and RCA CCDs were built on 10μm epi-layers and cannot be chem/mech thinned with good yields.

It has proven very difficult to obtain affordable working CCDs which can be thinned and operated at Steward Observatory. I have obtained several EEV P86115 setup grade devices. These have been thinned using the chemical-mechanical method with encouraging results. Figure 2.4 shows a quantum efficiency plot of the first chem/mech thinned setup grade EEV sensor both in the front and back illuminated mode. This data was taken using the CCD in a diode mode, where the QE is measured not on a pixel by pixel basis but by treating the whole device as one large pixel (Janesick 1987a). This test yields the same front illuminated QE for unthinned sensors as found by other researchers (Thorne *et al.* 1986). The poor blue and UV response is due to the large backside potential well of the untreated device. The TI sensor (not UV flooded) shows better blue response because of its smaller backside potential well, due to an oxide (unintentionally) grown on its surface some time after manufacture. Methods are discussed in Chapter 4 which are used to treat thinned devices to eliminate this backside well. It is interesting to note that the visible and red QE of the same CCD is higher when operated in the back illuminated mode than when front illuminated. This is due to the finite absorption of radiation of all wavelengths in the frontside electrode structure. When antireflection coatings are used, which cannot be applied to front illuminted devices (as discussed in Chapter 3), the QE of thinned devices is enhanced even more. Cosmic ray events are also reduced somewhat in thin devices. In fact, the only advantage of thick CCDs over properly optimized

thin devices is the absence of fringing. Even fringing, however, can be reduced to only a few percent in thin devices with the use of AR coatings optimized for the red.

Imaging with the setup grade EEV CCDs was not successful, due mainly to the low yield after thinning, mounting, and wire bonding. As indicated above, my early thinning efforts of these devices was targeted at 15μm or thinner, and several CCDs were destroyed when thinned to just less than 15μm. Only one setup quality device was successfully thinned and mounted, but images from the device were not obtained. This was due to poor wire bonding and subsequent electrical connection to Steward's CCD controller. The ultrasonic wire bonder to which I have access has proved to be unsuitable for bonding CCDs, and several devices have had their bonding pads destroyed with its use. A thermosonic gold ball bonder is suggested for these large devices and is presently on order. Valid quantum efficiency measurements have been made with thinned, non-functioning EEV CCDs as discussed above. These devices were received as mechanical samples and have shorted phases and/or damaged amplifiers. They do, however, allow for excellent QE measurement when operated in diode mode.

Through a collaboration with Photometrics, Ltd., in Tucson, I have been able to experiment with the thinning of several PM512 CCDs manufactured by Ford (Bredthauer *et al.* 1988). These devices have 516x516 20μm pixels and were designed for use as low light level sensors. They have a 15μm epitaxal layer, with my thinning goal being 15μm. These devices have never previously been succesfully thinned and have excellent potential as astronomical imaging devices. My thinning results with them have been very sucessful, although

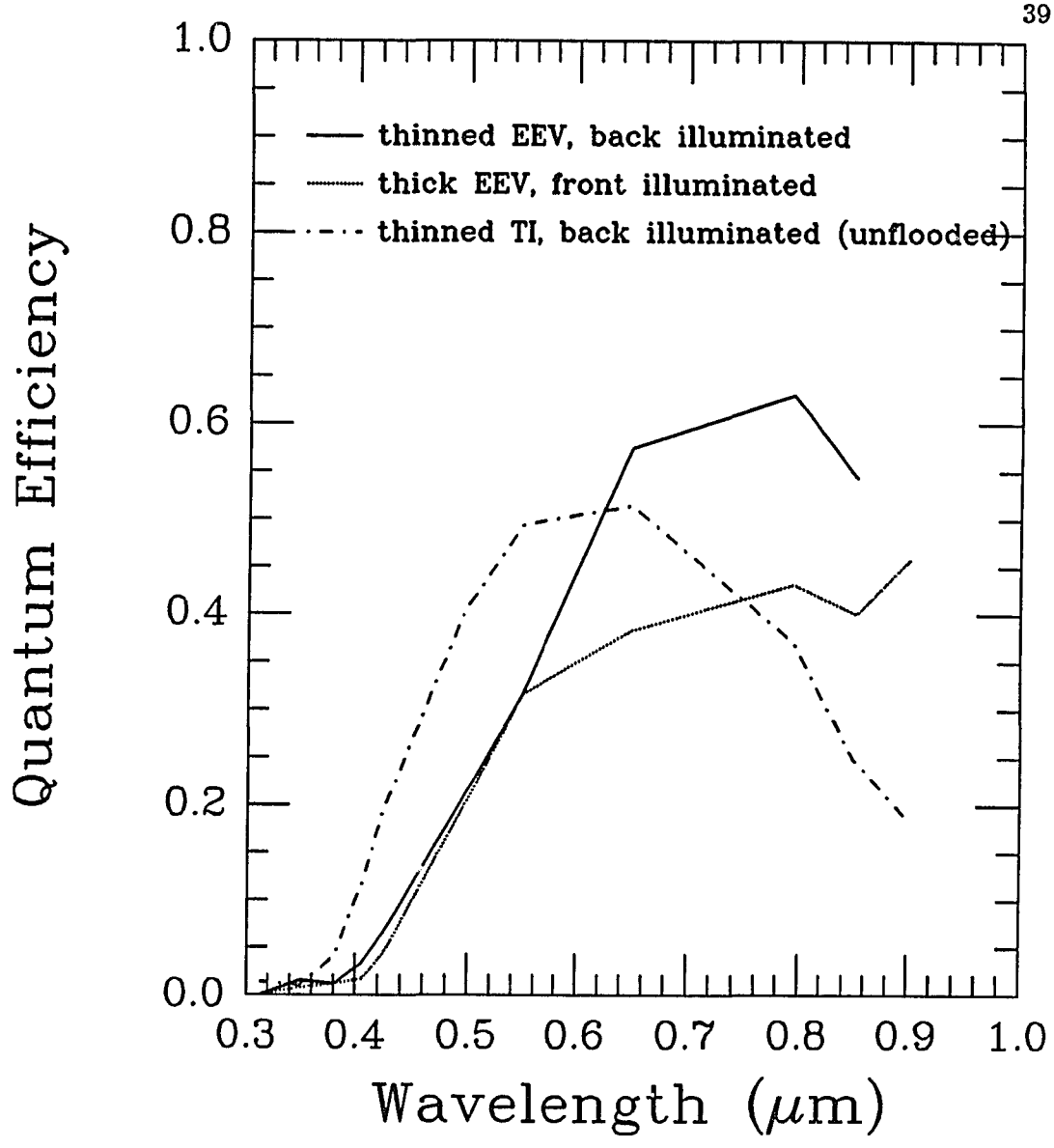

Figure 2.4. Quantum efficiency curves of three CCD's measured in the diode mode. The thinned EEV sensor is a setup grade device thinned at Steward using the chemical/mechanical process described in this chapter. There has been no attempt to grow an oxide layer or backside charge this device. It is mounted with its backside against a thin glass support. No AR coating has been applied. The thick EEV sensor is measured in the same diode manner using front illumination. The TI device's QE has been measured using the standard Steward QE measurement procedure in imaging mode, before a UV flood. It has better blue response due to a smaller backside potential well since it has a backside oxide. The thin EEV sensor is 15μm thick and therefore shows better red response than the 9μm TI sensor.

there is a serious problem associated with their lack of a substrate (ground) bonding connection.

The PM512 CCDs were designed to be operated in the front illuminated mode, or thinned with the acid etching technique used by Texas Instruments. This method thins the center region of the CCD only, and in fact the bonding pads of the device have been set away from the imaging area by 30μm. This eliminates edge effects caused by thinning variations and allows for fiber optic boule bonding, also planned for these devices. The edges of the imaging area on thinned devices should not show the "acid pooling" effect commonly seen in the TI 800x800 CCDs, where the edges of the image are thinner, have lower red response, and respond differently to UV flooding than the center. When the devices are acid thinned the edges remain thick and are able to act as the electrical connection to the substrate. The backside is coated with aluminum which makes an excellent ohmic contact to the non-polished silicon. The problem with this is that my chem/mech thinning method thins the entire backside and the aluminum connection is therefore thinned away. The highly polished Si surface does not allow for a quality electrical connection to the substrate, and thus the CCDs are very difficult to operate. I have sucessfully thinned and mounted several of these devices as shown in Figure 2.5, but sufficient charge transfer could not be obtained to produce an image. Electrical tests using an oscilloscope attached to the output amplifier show the device is operating correctly, but the missing ground connection is sufficient to not allow adequate potential wells to be clocked, and therefore to transfer charge. This fact has been confirmed by operating a thick device and then removing

the ground connection. Results of electrical tests are then identical with those of the thinned CCDs.

To demonstrate success of the chem/mech thinning method, I have mounted one PM512 CCD on an Invar frame with a square hole cut in the center of the same dimensions as the active imaging area of the CCD. After thinning, this frame was bonded to the CCD with conductive epoxy, allowing a relatively large surface area for electrical contact. Although the device is not mounted flat against glass as desired for a fully optimized detector, it is able to image successfully. Sufficient substrate contact was made with this technique, as shown by several images in Figure 2.6. This is in fact the first working, thinned PM512 CCD ever produced. Full characterization of this device will be obtained in the near future. Knowing that a backside contact is possible, my next step will be to deposit an aluminum contact on the non-imaging backside area and again mount the CCD on a transparent support substrate. Hopefully in the future these PM512 devices can be produced with a substrate contact (requiring a mask change), and the advantages of chem/mech thinning can be more easily obtained.

Future Thinning Requirements

An important thinning consideration involves the type of silicon wafer structures from which future CCDs will most likely be built. It was noted above that high resistivity devices allow deeper depletion depths (and therefore better red response and charge collection efficiency) and makes backside charging less difficult. If thick epitaxial layer devices of high resistivity are

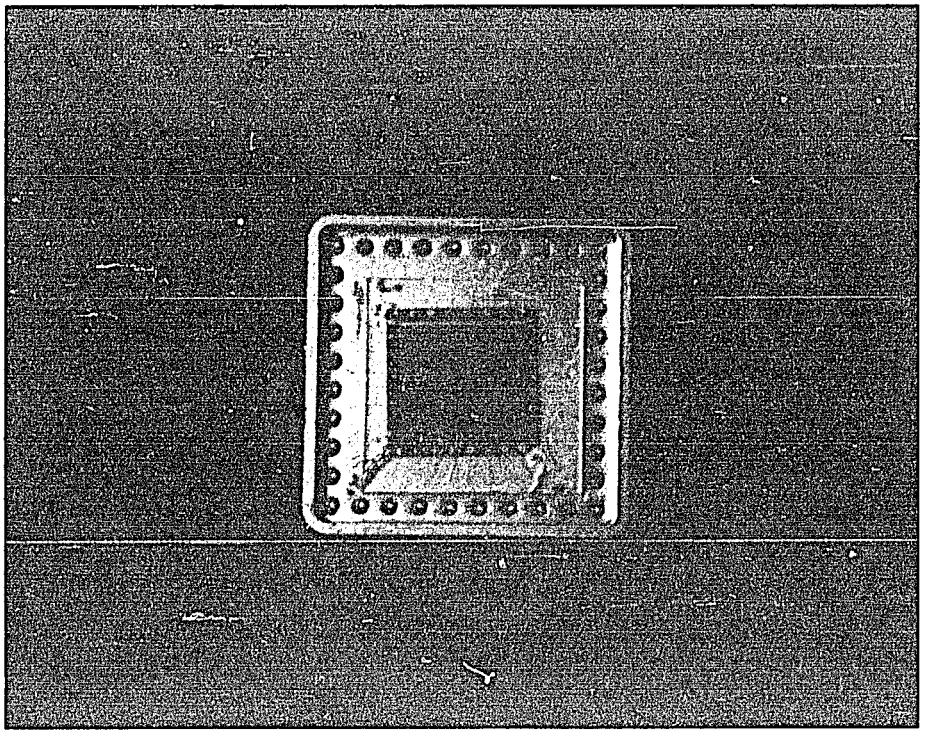

Figure 2.5. A 15μm thick Photometrics PM512 CCD after chem/mech thinning and mounting on a borosilicate glass support. The device hole cut in the Kovar device carrier is the size of the active imaging area. This device is functional, but unable to clock charge due to inadaquate substrate electrical conection as discussed in the text. The silver expoxy on the frontside is used to improve the wire bonding contacts and as an attempt to contact the silicon substrate.

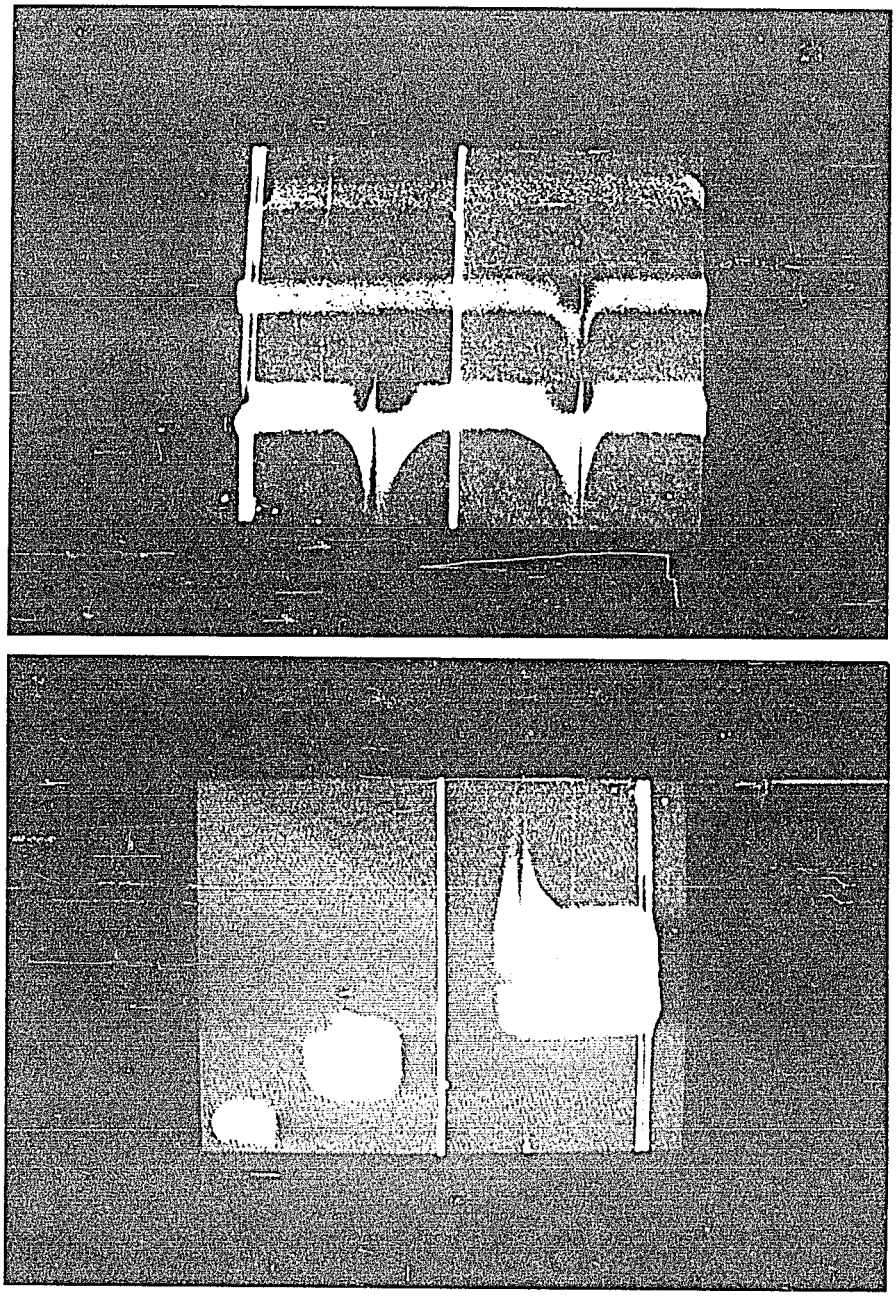

Figure 2.6. Two images taken a chem/mech thinned PM512 CCD. This device is 15μm thick and is mounted on an Invar frame to make a substrate ground connection. The top image is of three horizontal slits while the bottom image is of three rectangles. The vertical lines are three bad columns. There is a CTE problem in two regions of the device, possibly because the clocks voltages were not yet optimized. The images are not well focused due to the CCD location in a test dewar.

the way of the future, the thinning variations of acid etching may become less important for fully backside charged devices. For such devices acid thinning may be adequate, although not superior to chem/mech thinning. However, for producing mosaics of CCDs which require uniform, flat mounting and for thinning the wide variety of devices to which I realistically expect to have access in the next few years, chem/mech thinning is an excellent approach. It also has great potential for thinning entire wafers rather than single devices, which is of special interest to manufacturers. A particularly well suited application of chem/mech process would be the thinning of "buttable" CCDs. These devices have active imaging area extending to the silicon edge on one or more sides. The entire CCD must be thinned in this case – a very difficult task for acid solutions which would etch the edge of the CCD as well as the back surface.

Mounting CCDs

A major problem with thinned CCDs is the method currently used to mount them in their final package. The TI sensors are certainly unacceptably mounted for optimal use in optically fast beams, being supported only by the edges which allows excesive warpage. Steward's 90-inch CCD has an rms surface height variation of 30μm, with peak to valley deviations of 120μm. This has a direct impact on the quality of observations – in spectroscopic mode on-chip coaddition is often required to avoid defocus in the f/1.6 spectrograph beam. I have therefore found it necessary to develop a mounting technique that does not introduce image degradation due to surface ripple or movement.

Glass Support Substrate

The rippled surface seen on thinned CCDs is caused by stresses developed during thinning which are greater than those which the free silicon membrane can support. For this warpage to be significant, entirely thinned silicon must be less than 30μm thick. CCDs with thick borders do not show significant warpage unless thinned to less than about 15μm. Thicker devices show little surface warpage because the membrane is strong enough to support itself against the induced stresses. The simplest way to maintain a flat surface with thinner devices is to cement the device directly against a support substrate before releasing it from its thinning support. The support substrate used must match silicon's thermal expansion properties closely due to the frequent thermal cycling between room and operating temperatures (a 170°C differential). Because the wire bonds to the frontside bonding pads must be made after the detector is thinned (in order to allow a flat support for lapping and polishing), I have supported the chem/mech thinned CCDs with their backside against a borosilicate glass substrate. A similiar method has been used by RCA for their thinned CCDs. Incident radiation must therefore pass through this glass before being detected. Unfortunately this low expansion glass absorbs strongly below 3500Å, where CCDs still have high quantum efficiency. Corning Glass manufactures a UV transmitting borosilicate glass (9741) which may eliminate this problem. I have obtained a sample of this material and will produce a CCD support substrate from it in the near future. Thermal cycling tests have been conducted which demonstrate that it is possible to mount a thinned CCD on sapphire and cycle between room temperature and that of liquid nitrogen (−200°C). Although the expansion coefficient of these materials are quite dif-

ferent (Si has $\alpha \approx 3\text{x}10^{-6}$ while sapphire has $\alpha \approx 9\text{x}10^{-6}$), the thin silicon is put into compression against which it seems extremely durable. Sapphire is transparent to well below the atmospheric limit and is therefore also a suitable support material. A similiar mounting scheme was used by RCA for their back illuminated CCDs, although the glass support substrate was not UV transparent. Some devices have the glass support substrate removed (by etching) for increased UV response, but mechanical stress induced warping of the surface. In addition, many such devices have residual epoxy which was not removed in the etching and severely increased quantum efficiency nonuniformity.

In practice, the actual mounting of the CCDs requires great care to avoid breaking the thin silicon membrane. I have found the following technique to work well. Figure 2.7 shows a schematic view of the various CCD materials. Antireflection and transparent conductive coatings are applied to the CCD backside, as discussed in Chapters 3 and 4. An AR coating (MgF_2) is applied to the CCD support substrate on the side away from the CCD. Although the QE loss due to this surface is small, the coating helps to reduce fringing and ghost images. Several microns of cement are applied on the substrate which is then contacted to the CCD backside and cured. This cement must be transparent throughout the UV, visible, and near IR and not crack or lose adhesion at cryogenic temperatures. The cement must also remain slightly flexible (even when very cold) in order to relieve any thermal stresses developed due to the mismatched expansion coefficients of the silicon and glass. I use Epoxy Technology's 301-2 epoxy which meet these specifications very well. Once the cement is cured the assembly is gently heated to remove the thinning

support substrate. The CCD and support substrate are then mounted in a carrier and wire bonded for installation into a dewar.

Bump Bonding

An alternative mounting technique is to bond the CCD with its frontside against a support substrate. This can be done in two ways. It may be possible to cut small holes in the substrate for each wire bonding pad (about 200x200μm) and use a specially modified wire bonding machine to reach into these holes and make the wire bonds. However, after studying many methods of semiconductor packaging, I have concluded that the most promising technique is bump bonding, in which the frontside of the CCD is placed directly against a silicon substrate that has matching bonding pads for interconnections. Bump bonding is used for production mounting and bonding of many integrated circuits today, but not yet for devices are large as CCDs (Goldmann and Totta 1983). The bonding process consists of depositing metallic bumps on either the device to be bonded or the substrate used for support and electrical interconnection. These bumps must be composed of materials which will form reliable electric connection to both the metalization on the device and on the substrate (typically aluminum). Excellent results have been made in the past with indium bumps, using nickel, gold, and/or chromium as plating material to ensure wetting to aluminium. A bump bonding machine is used to align the device and substrate, and apply heat and/or pressure when necessary. Reflowing of the "solder" is often done in an oven after inital bumping to improve physical and electrical contact. This type of bump bonding is completely compatible with CCDs because of the low temperatures involved.

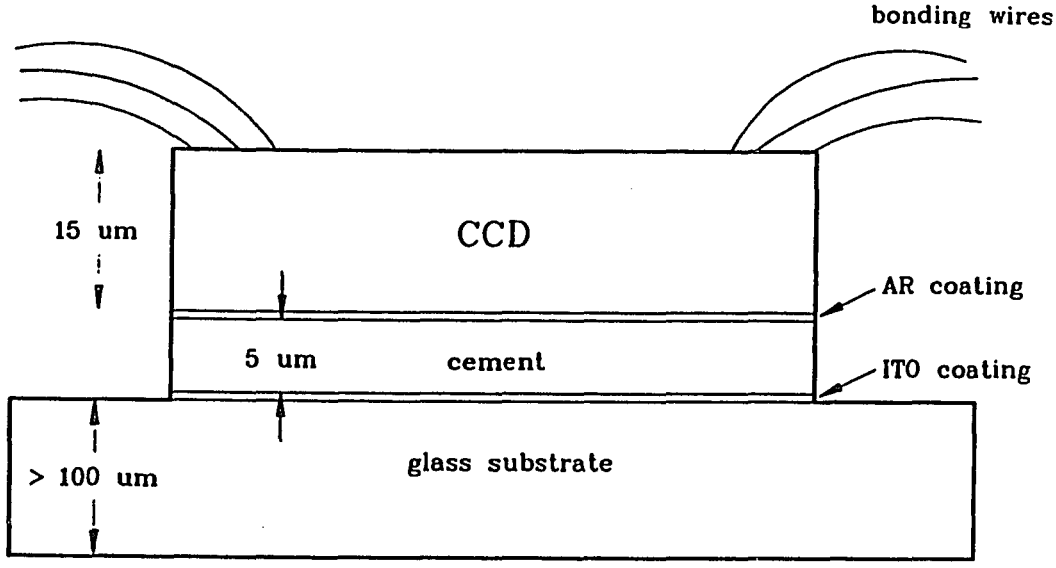

Figure 2.7. A schematic representation of a fully thinnned and optimized CCD as it is mounted ready for use. The header the device is wire bonded to is not shown since it may be either a single chip package or a mosaic device holder. The two thin films are less than 1μm thick. The wire supplying the voltage for backside charging contacts the Ag film or a metalisation on it with conductive epoxy. Many variations of this mounting system are possible, from a completely bare backside to this fully configured model. The thin films will be discussed in the following two chapters.

Although not yet demonstrated with CCDs, I believe this is the best method to mount thinned CCDs (especially for use in mosaics) and will work to develop this technique in the future. There are several important questions which must be researched to determine the feasibility of this bonding method for CCDs. The thermal effects of bonding devices as physically large as CCDs must be carefully studied, especially relating to thermal cycling from room temperature to that of liquid nitrogen. For reliable bonding, the proper metalization must exist on the device pads and on the bumps. If standard, commercially available CCDs are used the aluminum pads must be coated with another metal before bonding. One very important advantage of bump bonding is its application to CCD thinning. Using the chem/mech process where the entire CCD (or wafer) is thinned, bump bonding will allow electrical connection of devices before, during, and after the thinning process. CCDs could be bumped onto silicon support substrates and then thinned. They would not be removed from the support after thinning, which would increase the process yield. This bumping and thinning would require injection of epoxy under each device after electrical contact is made. This would provide support for the device during thinning as well as keep the imaging surface flat at all times, including during operation. Bump bonding also has no absorption problems since a glass support is not used on the backside. Because the devices would be mounted to a silicon substrate, no thermal expansion matching problems would arise. CCD bump bonding has the potential for making a major improvement in device packaging, and is essential for the production of large scale mosaics as will be discussed in Chapter 5.

CHAPTER 3

CCD ANTIREFLECTION COATINGS

One of the most significant quantum efficiency degradations of back illuminated CCDs is due to the large back surface reflection loss. The polishing required during the thinning process to minimize subsurface damage creates a mirror-like finish with an extremely high specular reflectivity. This reflection loss approaches 60% in the near UV, and remains greater than 30% throughout the visible and near IR, greatly reducing the CCD's quantum efficiency. In addition, "ghost" images are often formed when this reflected light is again reflected back to the detector by the dewar window or other optical elements. In the red and near IR, interference fringing modulates QE by as much as 20%, due to multiple reflections between the front and back surfaces of the CCD. The application of thin film antireflection (AR) coatings directly onto the CCD back surface can significantly reduce all of these problems. In this chapter I present a study of the materials and application methods required to produce such coatings. Both a theoretical description of the processes involved and results from laboratory experiments are discussed. Although a great deal of literature exists pertaining to AR coatings, no published studies have been made of the unique requirements of coatings for silicon CCDs, especially in the UV. Much of this work can also be found in Lesser (1987).

Figure 3.1 shows that the index of refraction n and extinction coefficient k of silicon increases strongly with decreasing wavelength in the blue and ultraviolet. The specular reflection from a polished silicon surface (such as a thinned back-illuminated CCD) in vacuum is given by $R = \left(\frac{\tilde{n}-1}{\tilde{n}+1}\right)^2$ for normal incidence, where $\tilde{n}$ is the complex refractive index of silicon ($\tilde{n} \equiv \mathrm{n} - i\mathrm{k}$). The resultant reflectivity from such a surface can be derived from Figure 3.3. The greatest QE improvement gained by AR coating is in the blue and UV, but a significant increase will also be obtained throughout the visible and near IR. In fact, since AR coatings can be optimized for any desired wavelength, a 50% to 100% QE enhancement may be realized at any wavelength from the atmospheric cutoff at 3100Å to the silicon response limit near 1μm.

Obtaining a significant quantum efficiency improvement requires that the AR coating be applied directly to the silicon surface. This is well suited for thinned, back illuminated CCDs in which the backside is exposed. The front surface of a CCD, however, is not exposed silicon but usually a protective glass covering (passivation) with a refractive index near 1.5. AR coatings on the frontside of a front illuminated CCD will therefore improve QE by a few percent at most. Substantial reflection losses occur at the interfaces between this passivation and the polysilicon gates, and between the gates and the underlying gate oxides. For these reasons the coatings described throughout this chapter are for thinned, back illuminated devices only. In the future, however, manufacturers may be able to replace the frontside passivation with a more suitable AR coating material to reduce some reflection loss for front illuminated sensors as well.

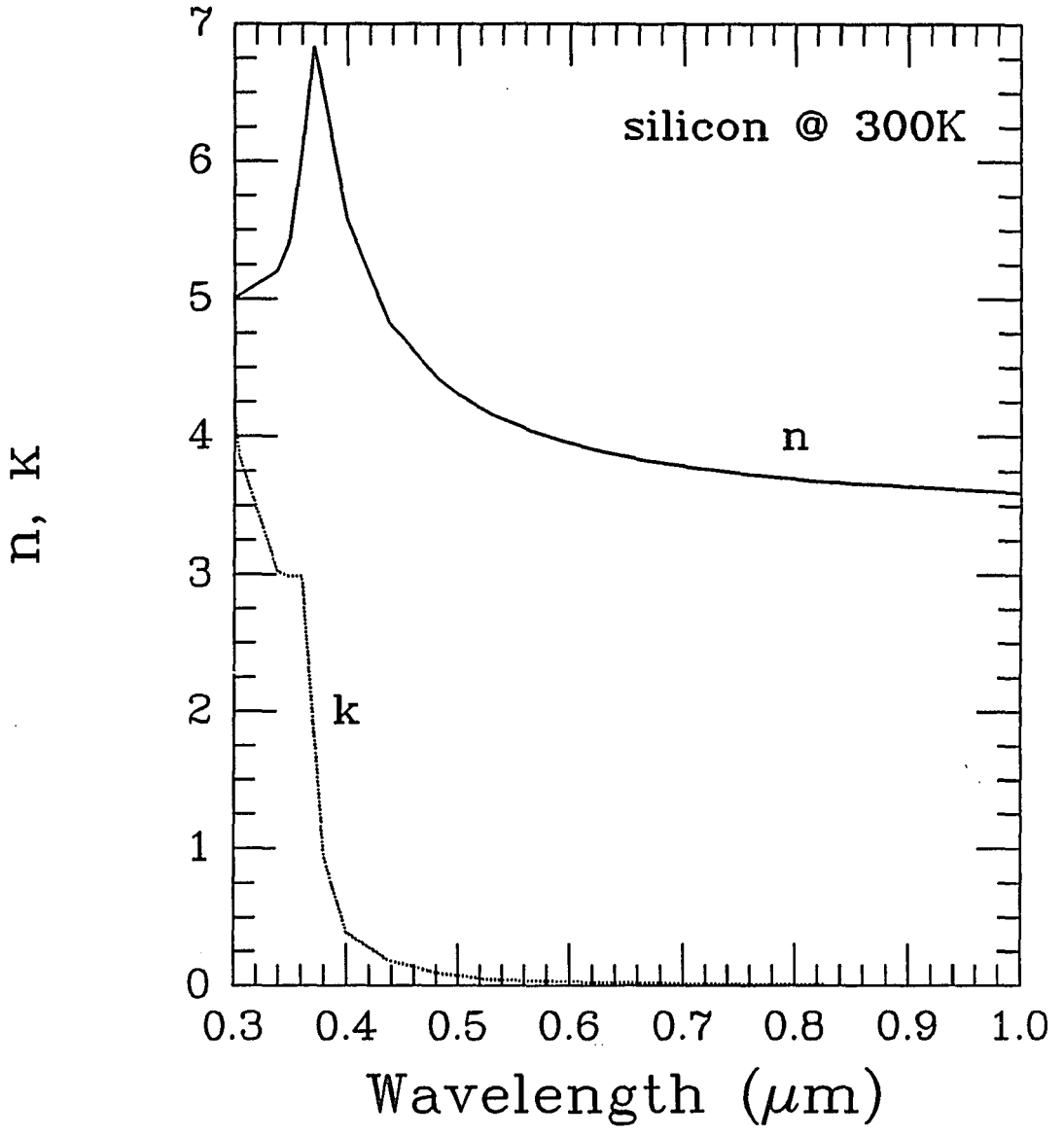

Figure 3.1. The optical constants of silicon at 300°K. The complex refractive index is $\hat{n} = n - ik$, where n is the refractive index and k is the extinction coefficient. The absorption coefficient α (reciprocal of the absorption depth) is given by $\alpha = \frac{4\pi k}{\lambda}$. The values of n and k are from Edwards (1985).

AR Coating Theory and Design

A thin film antireflection coating applied to an optical surface causes interference between the light reflected from the two sides of the thin film. By choosing suitable materials with the proper refractive indices, the amplitudes of the reflected wavefronts can be matched and near complete constructive and destructive interference obtained. By conservation of energy, any light not reflected or absorbed in this film must be transmitted into the substrate material, increasing the CCD's QE. The difficulty in designing such thin film systems for silicon is due to the large and varying refractive index and extinction coefficient of both silicon and the majority of suitable AR coating materials as a function of wavelength. A computer program is required to optimize the thin film system iteratively, taking into account the varying optical constants of all materials involved, incident light properties such as polarization and angle of incidence, and the phase changes associated with absorbing media.

Although simple thin film calculations to determine reflectance and transmittance for specific systems can be found in many references, the general case of an arbitrary number of absorbing films on an absorbing substrate (as needed for CCDs) is not easily solved. In this section I describe the method used to design the CCD AR coatings presented later. Absorption in the thin films and the substrate, variable optical constants, polarization state, angle of incidence, and an arbitrary number of layers are all allowed with this technique. All media are assumed to be homogeneous and isotropic. This method is based on a procedure described in Heavens (1965). The reflectance R and transmittance T of a system of thin films in terms of the incident,

reflected, and transmitted electric field amplitudes $\mathcal{E}_i$, $\mathcal{E}_r$, and $\mathcal{E}_t$ are given by

$$\mathrm{R} = \frac{\text{reflected energy}}{\text{incident energy}} = \left|\frac{\mathcal{E}_r}{\mathcal{E}_i}\right|^2 \qquad \text{and}$$

$$\mathrm{T} = \frac{\text{transmitted energy}}{\text{incident energy}} = \mathrm{Re}\left(\frac{n_{k+1}}{n_0}\right)\left|\frac{\mathcal{E}_t}{\mathcal{E}_i}\right|^2$$

since the energy in a radiation field is given by the Poyting vector $\mathbf{S} = \frac{c}{4\pi}\left|\mathbf{E}\times\mathbf{H}\right| = \frac{c}{4\pi}|\hat{n}||\mathbf{E}|^2$ where $\mathbf{E}$ and $\mathbf{H} = \hat{n}\mathbf{E}$ are the electric and magnetic field intensities, respectively. The amplitudes and indices of each medium in a system of k thin film layers will be labeled with a subscript ranging from 0 for the incident medium to $k+1$ for the substrate.

Multiple interference from radiation reflected from all media interfaces is allowed for if E_j^+ is defined as as the total tangential electric field amplitude in the j^{th} media moving in the direction of propagation, and similiarly E_j^- in the opposite direction, as shown in Figure 3.2. The total tangential magnetic field intensity amplitudes H_j^+ and H_j^- is defined in the same way. Therefore, for light polarized with its electric field vector in the plane of incidence (p-polarized),

$$E_j^\pm = \mathcal{E}_j^\pm \cos\phi_j \qquad \text{and} \qquad H_j^\pm = \pm\hat{n}_j\mathcal{E}_j^\pm = \pm\hat{n}_j\frac{E_j^\pm}{\cos\phi_j}$$

where $\mathcal{E}_j^\pm$ is the total electric field amplitude at the $(j, j+1)$ interface moving in the positive $(+)$ or negative $(-)$ direction. The angle ϕ_j is the angle of incidence of radiation at the $(j, j+1)$ interface measured from the normal. With $\mu_j = \frac{\hat{n}_j}{\cos\phi_j}$ then $H_j^\pm = \pm\mu_j E_j^\pm$. The same formulae can be used for radiation polarized perpendicular to the plane of incidence (s-polarized) if for this case $\mu_j = \hat{n}_j\cos\phi_j$. Any arbitrary polarization angle can, of course, be obtained through a linear superposition of these two polarization states.

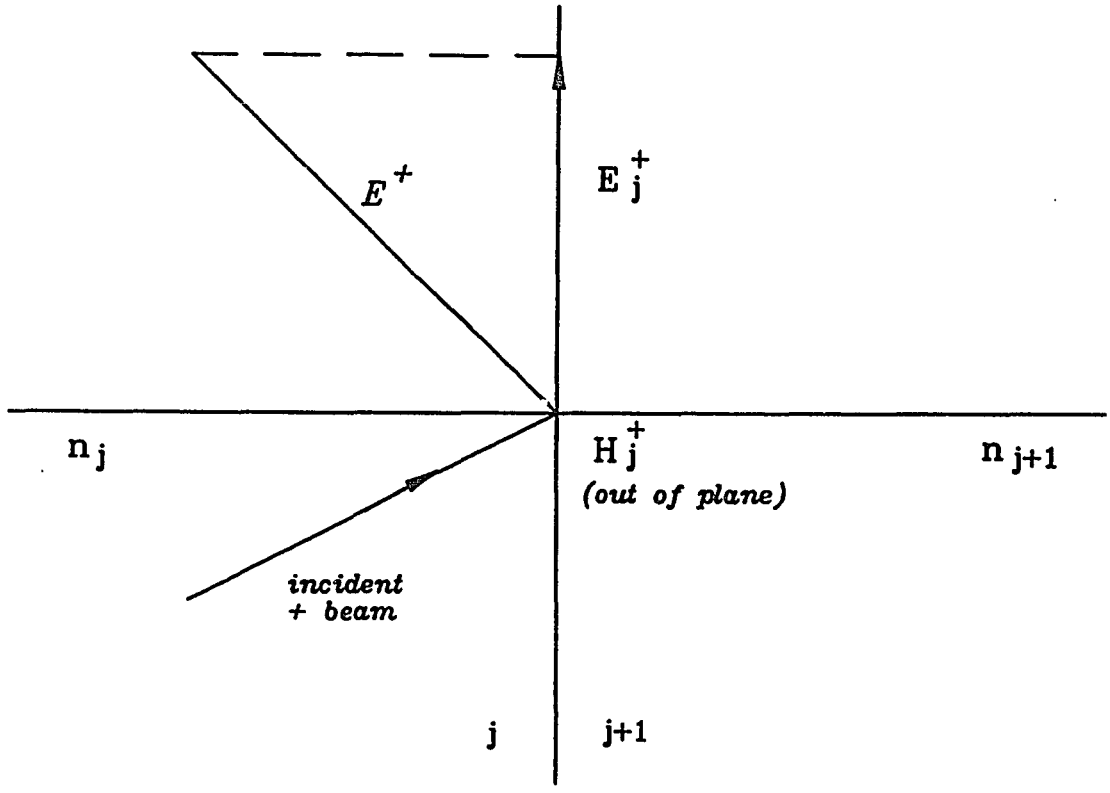

Figure 3.2. Definitions used in the derivation of the general equations for reflectance and transmittance of an absorbing thin film stack. The radiation is initially moving in the + direction.

Since the tangential components of $\mathbf{E}$ and $\mathbf{H}$ must be continuous across an interface of two media according to Maxwell's equations,

$$E_{j-1}^{+} + E_{j-1}^{-} = E_j^{+} \exp ig_j + E_j^{-} \exp -ig_j \qquad \text{and}$$

$$H_{j-1}^{+} + H_{j-1}^{-} = H_j^{+} \exp ig_j + H_j^{-} \exp -ig_j \qquad \text{or}$$

$$\mu_{j-1}(E_{j-1}^{+} - E_{j-1}^{-}) = \mu_j\left(E_j^{+} \exp ig_j - E_j^{-} \exp -ig_j\right)$$

where $g_j = \frac{2\pi}{\lambda}\hat{n}_j t_j \cos\phi_j$ is the phase change of the radiation of wavelength λ as it traverses layer j of physical thickness t_j.

These equations can be used to form a recursive relation in terms of the total tangential field intensities $E_j = E_j^{+} + E_j^{-}$ and $H_j = H_j^{+} + H_j^{-}$. By expanding the exponetials above in terms of sines and cosines and substituting E_j and H_j,

$$E_{j-1} = \cos g_j E_j + \frac{i \sin g_j}{\mu_j} H_j \qquad \text{and}$$

$$H_{j-1} = i\mu_j \sin g_j E_j + \cos g_j H_j.$$

Written in matrix form, this becomes

$$\begin{pmatrix} E_{j-1} \\ H_{j-1} \end{pmatrix} = \begin{pmatrix} \cos g_j & \frac{i \sin g_j}{\mu_j} \\ i\mu_j \sin g_j & \cos g_j \end{pmatrix} \begin{pmatrix} E_j \\ H_j \end{pmatrix}.$$

The tangential electric and magnetic field amplitides in the incident medium and the last thin film are therefore related by

$$\begin{pmatrix} E_0 \\ H_0 \end{pmatrix} = \mathbf{M_1 M_2 ... M_k} \begin{pmatrix} E_k \\ H_k \end{pmatrix} \equiv \mathbf{M} \begin{pmatrix} E_k \\ H_k \end{pmatrix}$$

where $\mathbf{M}_j$ is the above recursion matrix for layer j. The matrix elements m_{11}, m_{12}, m_{21}, and m_{22} can be easily computed with a suitable computer program given the angle of incidence, complex index of refraction at all wavelengths needed, and the thickness of each layer in the system. The reflectance

and transmittance can then be found as follows.

$$E_0 = m_{11}E_k + m_{21}H_k = m_{11}E^+_{k+1} + m_{21}\mu_{k+1}E^+_{k+1} \qquad \text{and}$$

$$H_0 = m_{12}E_k + m_{22}H_k = m_{12}E^+_{k+1} + m_{22}\mu_{k+1}E^+_{k+1}$$

since $E_k = E^+_{k+1}$ and $H_k = H^+_{k+1} = \mu_{k+1}E^+_{k+1}$, as $E^-_{k+1} = 0$. Therefore,

$$\mathrm{T} = \mathrm{Re}\left(\frac{n_{k+1}}{n_0}\right)\left|\frac{\mathcal{E}^+_{k+1}}{\mathcal{E}^+_0}\right|^2 = \mathrm{Re}\left(\frac{n_{k+1}}{n_0}\right)\left|\frac{E^+_{k+1}}{E^+_0}\right|^2\left(\frac{\cos\phi_0}{\cos\phi_{k+1}}\right)^2$$

$$= \mathrm{Re}\left(\frac{n_{k+1}}{n_0}\right)\left|\frac{2\mu_0}{m_{11}\mu_0 + m_{21}\mu_{k+1}\mu_0 + m_{12} + m_{22}\mu_{k+1}}\right|^2\left(\frac{\cos\phi_0}{\cos\phi_{k+1}}\right)^2$$

and

$$\mathrm{R} = \left|\frac{\mathcal{E}^-_0}{\mathcal{E}^+_0}\right|^2 = \left|\frac{E^-_0}{E^+_0}\right|^2 = \left|\frac{m_{11}\mu_0 + m_{21}\mu_{k+1}\mu_0 - m_{12} - m_{22}\mu_{k+1}}{m_{11}\mu_0 + m_{21}\mu_{k+1}\mu_0 + m_{12} + m_{22}\mu_{k+1}}\right|^2.$$

The models presented below for CCD antireflection coatings have been calculated from these expressions for R and T.

Material Selection

Once the computation algorithm has been developed to design AR coatings, appropriate thin film materials must be found. After considering the properties required of a CCD AR coating, and the many possible application methods, I have found there are two two general classes of constraints which limit the production of such coatings. These are material constraints which depend on the thin film materials themselves, and application constraints which depend on the techniques used to apply these coatings to CCDs. I discuss these below.

Material Constraints

Refractive Index. The most significant material constraint is that thin film materials of very high index of refraction be used in order to make a good "impedance" match between the incident medium (taken here as a vacuum) and silicon. An ideal single layer coating for use at normal incidence, optimized for a wavelength λ, requires a refractive index $n(\lambda) \approx \sqrt{n_{Si}(\lambda)}$, where n_{Si} is the refractive index of silicon. A coating material with $n \approx 2.4$ in the UV or $n \approx 2$ in the visible and near infrared is needed to obtain zero reflection at the wavelength of optimization. There are few transparent materials with such a large refractive index, and none whose index increases as rapidly in the UV as necessary to match silicon. In comparision, an AR coating used to obtain zero reflection from a glass surface requires only $n \approx 1.33$. This requirement is met fairly well by materials such as magnesium fluoride, chiolite, and cryolite. No material exists which optimally meets all the requirements for a CCD AR coating usable from the UV to the IR. It is therefore necessary to make compromises in the design which allow a coating to provide the most useful QE boost for the applications of any particular sensor.

Absorption Coefficient. I have set a design goal of achieving greater than 80% transmission into silicon over the spectral region from 0.31μm to 1.0μm. Unfortunately, the majority of high index materials commonly used in thin film systems are strong absorbers in the UV. For example, a common choice for silicon AR coatings in the visible is silicon monoxide (SiO), which is often used on solar photocells. SiO has an index near 1.9 in the visible but a quarter wave layer optimized for 4000Å absorbs 37% of the incident 3500Å

light. Other common high index coating materials which cannot be used due to high UV absorption include ZnS, TiO, TiO_2, and CeO_2.

Radioactivity. Because high energy particles can create long trails of electron-hole pairs in silicon, CCDs are quite sensitive to radioactivity. Cosmic ray detections cannot be avoided but must be removed with image processing techniques. Local sources of radioactivity, however, can often be eliminated by adaquate selection and testing of the materials used near the detector. Thorium compounds in particular are common in thin film systems but may not be used with CCDs due to their radioactivity.

Stress. The stress developed in thin films can be extremely high in many cases. Deposited films are usually in tension due to thermal mismatch when the hot coating material is applied to a relatively cool substrate. The film cools after application but is unable to contract due to adhesion to the substrate, creating tension stress. Because back illuminated CCDs are typically thinned to less than twenty microns, these high stress films can actually warp the detector. For many applications, especially when using a fast focal ratio, only a small amount of surface curvature can be tolerated before the optical performance of the system is significantly degraded. Warping by 30μm causes nearly half the light from a point source to be lost to adjacent pixels due to defocus, assuming 15μm pixels in an f/1 beam. This problem is especially detrimental to spectroscopic applications where such fast focal ratios are common. While most films do not develop such high stresses, magnesium fluoride (the most common low index coating material) is capable of warping a thinned

CCD ten times more than this (Ennos 1966). Clearly this material should not be used for CCDs which are not well supported across their entire surface.

Application Constraints

Temperature. Since AR coatings are applied after CCDs are manufactured (and thinned), excessive heating can damage the metalizations used for electrical conduction in the device (usually aluminum). Most manufacturers recommend that CCD temperatures remain below 200°C to avoid danger. This requires that the coating system used to apply AR films be fitted with a heat shielding shutter and that an electron beam gun rather that a resistive heating element be used to evaporate those materials with very high evaporation temperatures. This will reduce CCD heating during the coating process. Most chemical deposition techniques require that the substrate and films be baked at high temperatures (> 400°C) to produce a final transparent coating. Some evaporated films must also be applied to heated substrates to improve their durability and adhesion. Neither of these techniques are allowable when coating CCDs.

Lattice Damage. Semiconductors are susceptible to radiation damage from high energy photons and particles, causing lattice defects which result in excessive noise during operation. Sputtering is a common thin film application method which must be avoided or carefully controlled when used for coating CCDs. During sputtering, a strong electric field is produced in the coating chamber that accelerates ions to a target of the desired coating material. Through momentum transfer target molecules are knocked free and travel to the substrate (CCD). These high energy molecules or ions can easily damage

the CCD lattice structure. Careful shielding is necessary to protect the CCD if sputtering is required. Thermal or electron beam evaporation techniques involve much lower energy particles and present less possibility of damage to the lattice. For the coatings discussed here, only thermal evaporation with a heat shielding shutter has been used.

Suitable Materials

Given these constraints, there are few suitable materials that can be used for efficient CCD AR coatings. These include hafnium oxide (HfO_2), aluminum oxide (Al_2O_3), and lead fluoride (PbF_2). Of these, HfO_2 has the highest index of refraction and is the most promising candidate for a single layer coating. PbF_2 is also an excellent choice which requires a considerably lower evaporation temperature (400°C) than HfO_2 (2500°C) and therefore presents less danger to the CCD. All of these materials are readily available from major thin film material suppliers and have very stable properties. Tantalum pentoxide (Ta_2O_5) and zirconium oxide (ZrO_2) may also be suitable materials for CCD AR coatings but their optical constants vary tremendously with application method.

Multilayer AR coatings on silicon require both high and low refractive index films. The same constraints discussed above apply to these materials. Fortunately, there are several suitable low index dielectrics which are transparent in the UV. Magnesium fluoride, cryolite (Na_3AlF_6), and chiolite ($Na_5Al_3F_{14}$) are low index, low absorption materials commonly used in AR coatings. MgF_2 is unsuitable for unsupported CCDs due to its high internal stress. Chiolite ($n = 1.33$) can usually be obtained with higher purity and more stable opti-

cal and mechanical properties than cryolite and I have used it as the design material for the low index films in the multilayer systems described below.

The following references contain the optical constants for the materials discussed here: Si (Edwards, 1985), SiO (Philipp, 1985), HfO_2 (Smith and Baumeister, 1979), Al_2O_3 (Malitson, 1962), and PbF_2 (Driscoll, 1978).

Modeling Results

The coating designs produced from the above materials are listed in Table 3.1, and their efficiencies as a function of wavelenth are shown in Figures 3.3 and 3.4. The ordinate in these figures must be multiplied by the internal quantum efficiency of a given CCD (the probability of detection of a photon which has penetrated the silicon surface) to obtain the actual QE of a coated detector. It is important to maximize transmission into the CCD when dealing with absorbing materials rather than to minimize reflection. Because of phase changes at the interfaces of the thin films, the wavelengths for these two occurences will be different. Minimum reflection is obtained with a different coating thickness than maximum transmission. For optimizing detector QE, maximum transmission is certainly desired.

Single Layer Coatings

From the single layer coatings shown in Figure 3.3 it can be seen that HfO_2 is the best material for use in the UV due to its high index of refraction. One coating is shown which is optimized in the visible, at 0.55μm, rather than in the UV as are the others. Although the efficiency of this coating is

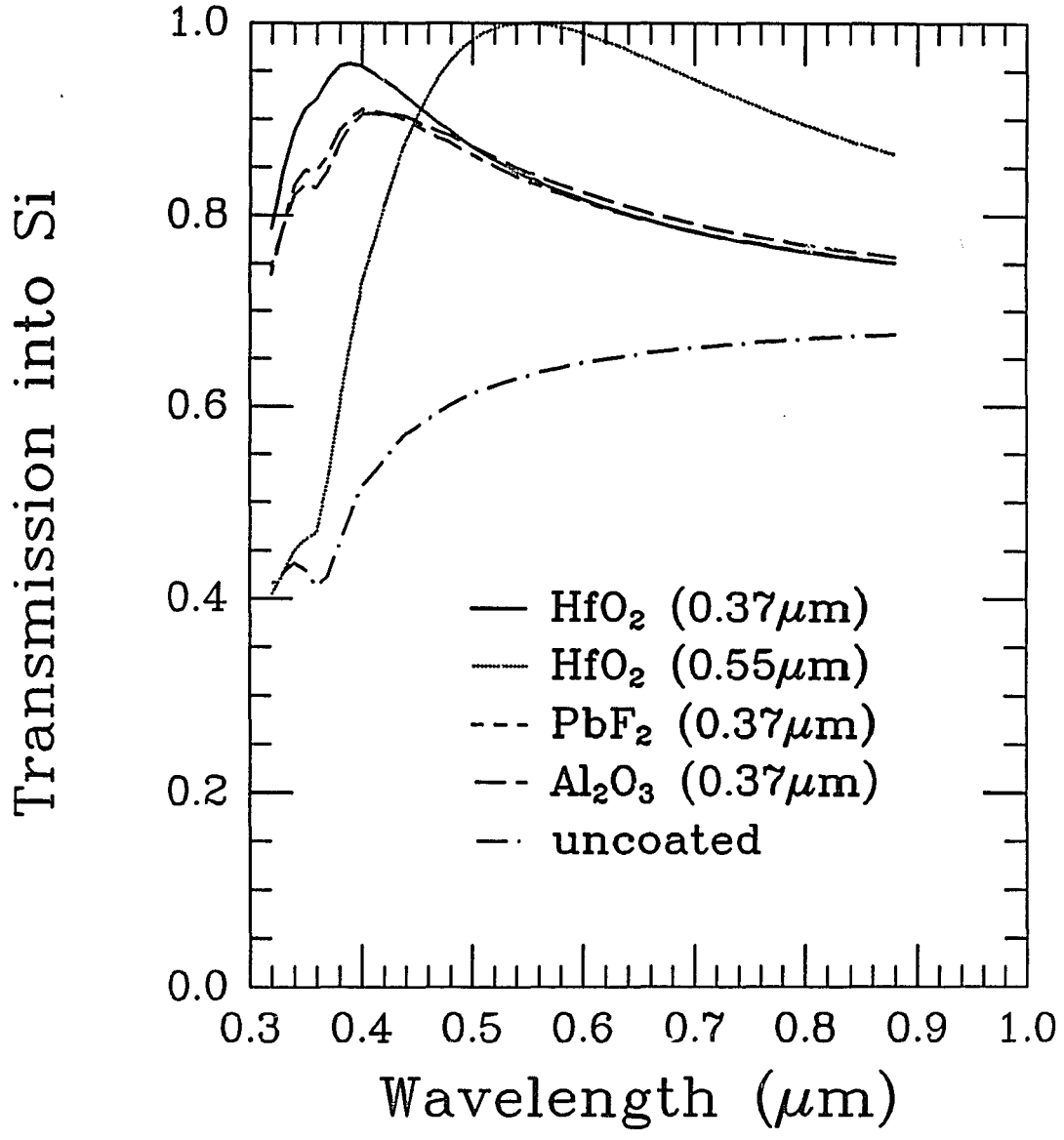

Figure 3.3 Calculated single layer antireflection coatings for a silicon CCD. The wavelength of optimiztion is given with the material name. The thickness of each coatings is listed in Table 3.1. Absorption by the coating and substrate is included.

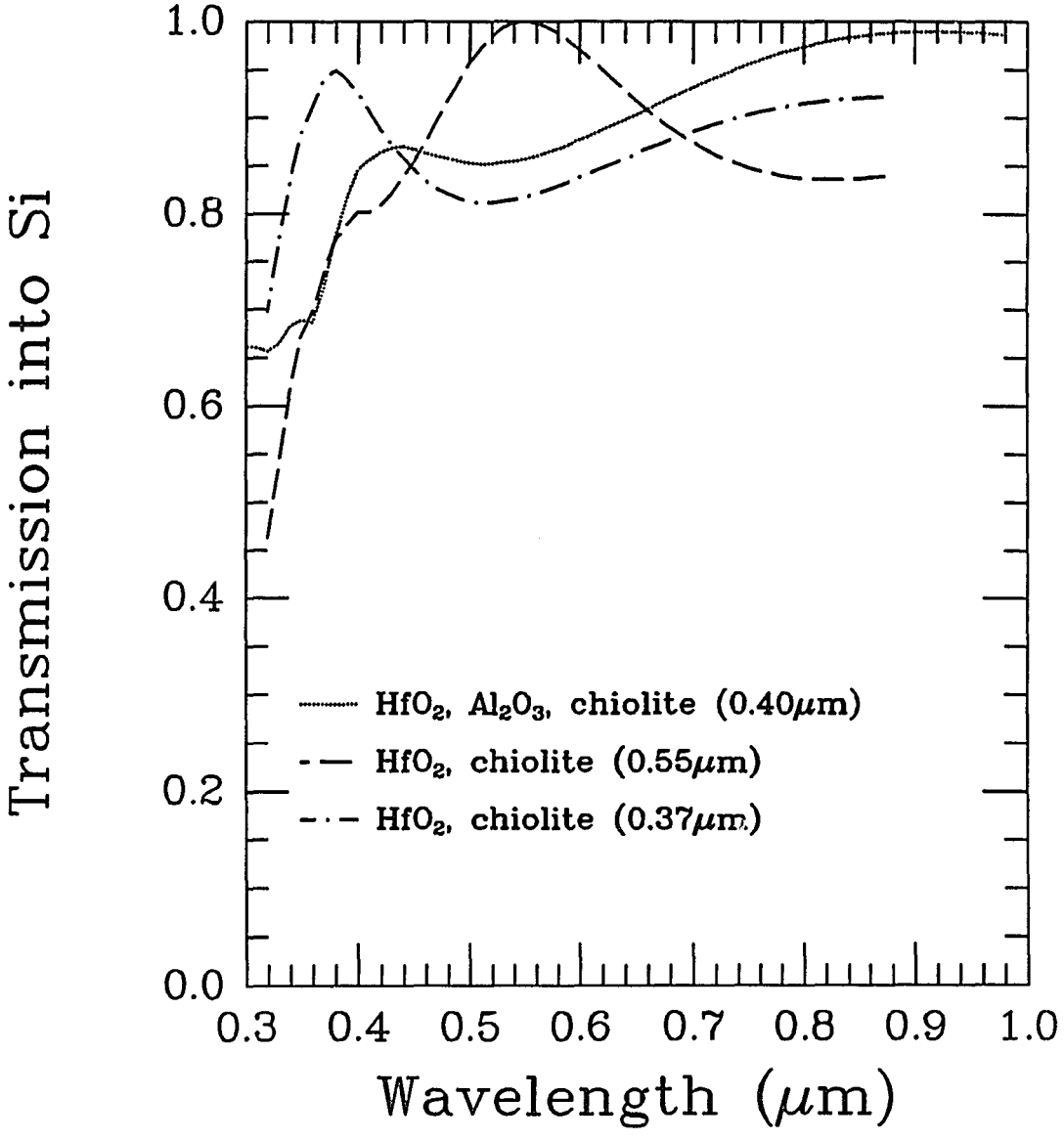

Figure 3.4 Calculated multilayer antireflection coatings for a silicon CCD. The wavelength of optimiztion is given with the material name. The thickness of each coatings is listed in Table 3.1. Absorption by the coating and substrate is included.

TABLE 3.1

Antireflection Coating Parameters

Material	*Thickness (Å)*	*Optimized λ (μm)*
HfO_2	410	0.37
PbF_2	478	0.37
Al_2O_3	491	0.37
HfO_2	671	0.55
HfO_2, chiolite	410, 1391	0.37
HfO_2, chiolite	634, 2221	0.55
HfO_2, Al_2O_3, chiolite	476, 559, 752	0.55

about 15% higher at this wavelength, the UV efficiency is reduced by 40% at 0.32μm. In all cases, coatings which are optimized in the visible show significant degradation in the UV due to silicon's rapid increase in refractive index toward shorter wavelengths. Coatings optimized in the UV are much less degraded in the visible and red and are preferred because their higher broadband QE improvement. addition, In because silicon's refractive index is considerably lower in the red, a smaller QE boost will be obtained since the absolute reflection loss is nearly 30% less than in the UV. I have found that the best broadband AR coatings should be optimized near 0.37μm. This is near the wavelength of maximum reflection loss for silicon and therefore where the greatest gain in QE can be obtained. Astronomically it is also near the central wavelength of the Johnson U photometric filter (λ = 3650Å). Optimizing QE in this region is important for many photometric observational projects.

Multi-layer Coatings

Figure 3.4 shows the efficiencies of several multi-layer coatings consisting of HfO_2 and chiolite. None of these coatings are significantly better than the single layer HfO_2 coating for wavelengths less than about 0.6μm. The choice between the single and multi-layer coatings will depend on the particular application for which the detector is intended. In the case of a general purpose detector, the single layer coatings perform well and are simplest to apply.

Figure 3.5 compares the predicted QE of one of Steward's TI CCDs with a single quarter-wave HfO_2 coating and with the two layer HfO_2 + chiolite coating, both optimized at 0.37μm. The measured QE of the uncoated device is also shown. These predicted performance curves assume that the same internal QE of this sensor can be obtained using flash gate or conductive coatings as are presently obtained with the UV flooding technique (see Chapter 4). Recent laboratory experiments have demonstrated this to be true with both techniques. As expected, the multilayer AR films provide a higher peak efficiency and should be used when a detector is mainly intended for observations in a specific spectral region.

Other two and three layer coatings have also been designed but show no significant advantages over the coatings presented here. In general, multilayer coatings allow higher QE at certain wavelengths, but oscillate rapid to yield lower QE in many regions. It should be noted silicon multilayer AR coatings do not show the traditional multiple minima seen, for instance, when such systems are applied to glass, because of rapid changes in silicon's refractive

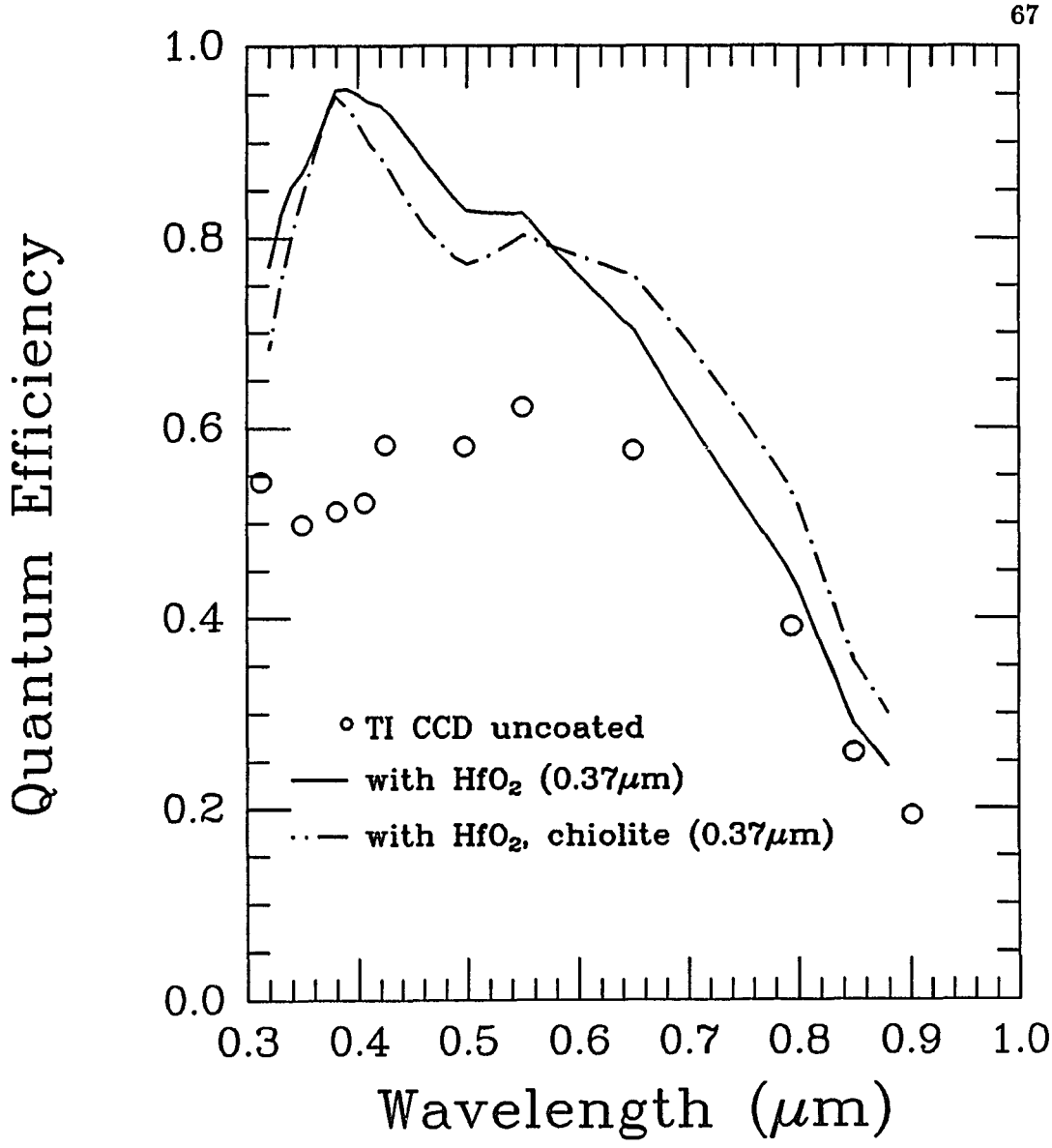

Figure 3.5. The predicted quantum efficiency of one of Steward Observatory's 800x800 3-phase CCD with AR coatings. It is assumed that the internal QE of the device is the same as currently obtained using a UV flood to eliminate the backside potential well. A flash oxide/gate or a conductive coating must therefore be used instead of flooding as discussed in the text.

index in the UV. If coatings were designed only for the visible and near IR, the standard shapes would be obtained.

Laboratory Results

Figure 3.6 shows a comparison of predicted and actual quantum efficiency improvement for an AR coated silicon photodiode. As can be seen, the QE gain is dramatic and in good agreement with the models. The differences can be accounted for by variations in the optical constants between values found by other researchers (and used in the models presented here) and those in the films actually applied. Factors which affect n and k include substrate temperature, residual gas pressure and composition, the rate of deposition of the films, and substrate surface conditions. These results demonstrate that excellent QE improvement can be obtained by relatively simple means. As long as the vacuum chamber used to apply the coatings offers sufficient protection from heat and high energy particles, and gas adsorption is not needed for backside charging, AR coatings should be used for all back illuminated CCDs. The risk in coating these detectors is extremely small while the benefit is substantial. There are no other detector optimization techniques (including thinning) which can offer such dramatic QE improvement over such a wide spectral region.

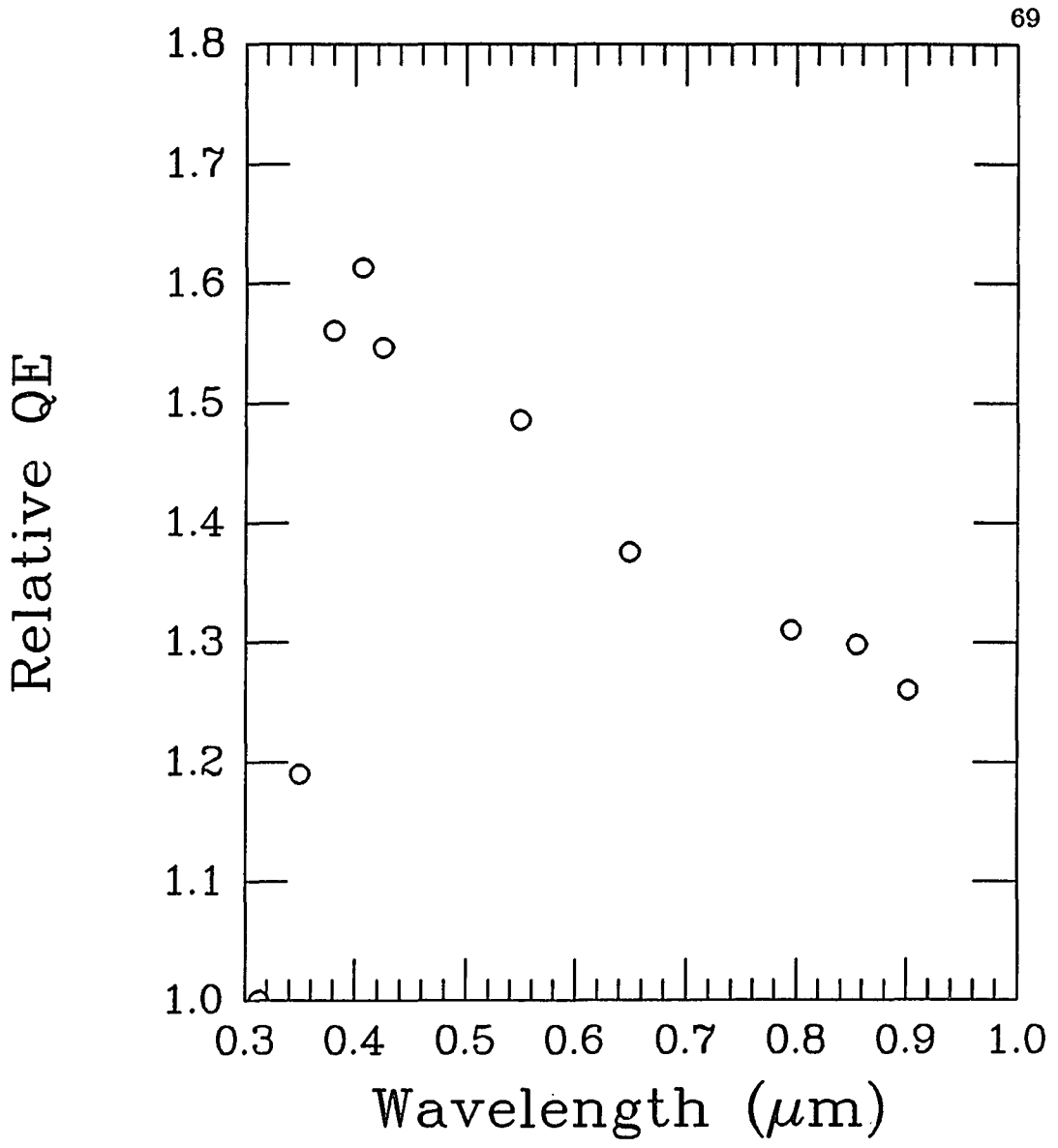

Figure 3.6. The measured quantum efficiency improvement of a silicon photodiode after application of PbF_2 antireflection coatings. The coating is 560Å thick, optimized for $\lambda =$ 4100Å.

Fringing

Fringing is an interference effect which causes substantial QE variations in thinned CCDs used in the red. It is produced by constructive and destructive interference of light multiply reflected between the front and back surfaces of a thinned device. Because silicon's absorption length is very short in the visible and UV, fringing occurs only longward of about 7000Å for most CCDs where light is reflected several times in a CCD before being absorbed. Thinner CCDs will show worse fringing due to the smaller absorption between internal reflections. The resultant QE of each pixel is determined by the wavelength of light and actual thickness of the detector at that pixel. Since thickness typically varies by many light wavelengths over a CCD, the effective QE even for monochromatic light will vary substantially. Fringing is most noticable in spectroscopy but also is a problem for direct imaging when using narrow-pass filters and due to bright night-sky emission lines. Sky fringing is an additive effect which can be well subtracted from data frames only if the sky line intensity ratios are fairly constant with time. Spectroscopic fringing from object or sky can in theory can be easily corrected since each pixel should always be illuminated by the same color. However, the very rapid pixel-to-pixel and intra-pixel QE variations make fringing extremely sensitive to instrument flexure. Fringe amplitudes are typically 10% of the mean signal and a means of reducing this for back illuminated CCDs would be great benefit to nearly all observations in the red and near-IR.

There are two methods of decreasing the QE variations caused by fringing. One is uniform thinning so thickness variations become unimportant.

Since a thickness change of only a quarter-wave ($\approx$ 2000Å) is enough to modulate QE from minimum to maximum, extremely precise thinning is required. The chem/mech technique is capable of such precision locally, but some amount of tilt ($\approx$ 5000Å) will always present. This only introduces a large spatial scale QE variation which is much easier to remove with data reduction techniques than fringing due to rapid local thickness variations. Another, more effective method of reducing fringing is the application of AR coatings. By reducing the reflection at the back surface of a CCD, the amplitude of the fringes will be substantially reduced. This is simply because less light is multiply reflected inside the CCD to cause interference. Figure 3.7 showns the predicted effect of AR coatings on fringing amplitudes. The single layer HfO_2 coating applied in this model reduces fringing amplitudes by more than 75% (to less than 2%) as well as increases the mean QE by 30%. Since fringing is the major drawback of using thinned CCDs in the red, the application of these coatings is extremely important for more efficient use of CCD detectors.

AR Coatings and Backside Charging

Antireflection coatings must be used in conjunction with backside charging techniques which direct photoelectrons away from the back surface and toward the frontside collection wells to obtain maximum QE. A number of methods (discussed fully in Chapter 4) such as flash gates and conductive films are under development which are compatible with AR coatings. Techniques requiring atomic or molecular adsorption on the silicon surface such as UV flooding or nitric oxide gas treatments cannot be used because the thin film

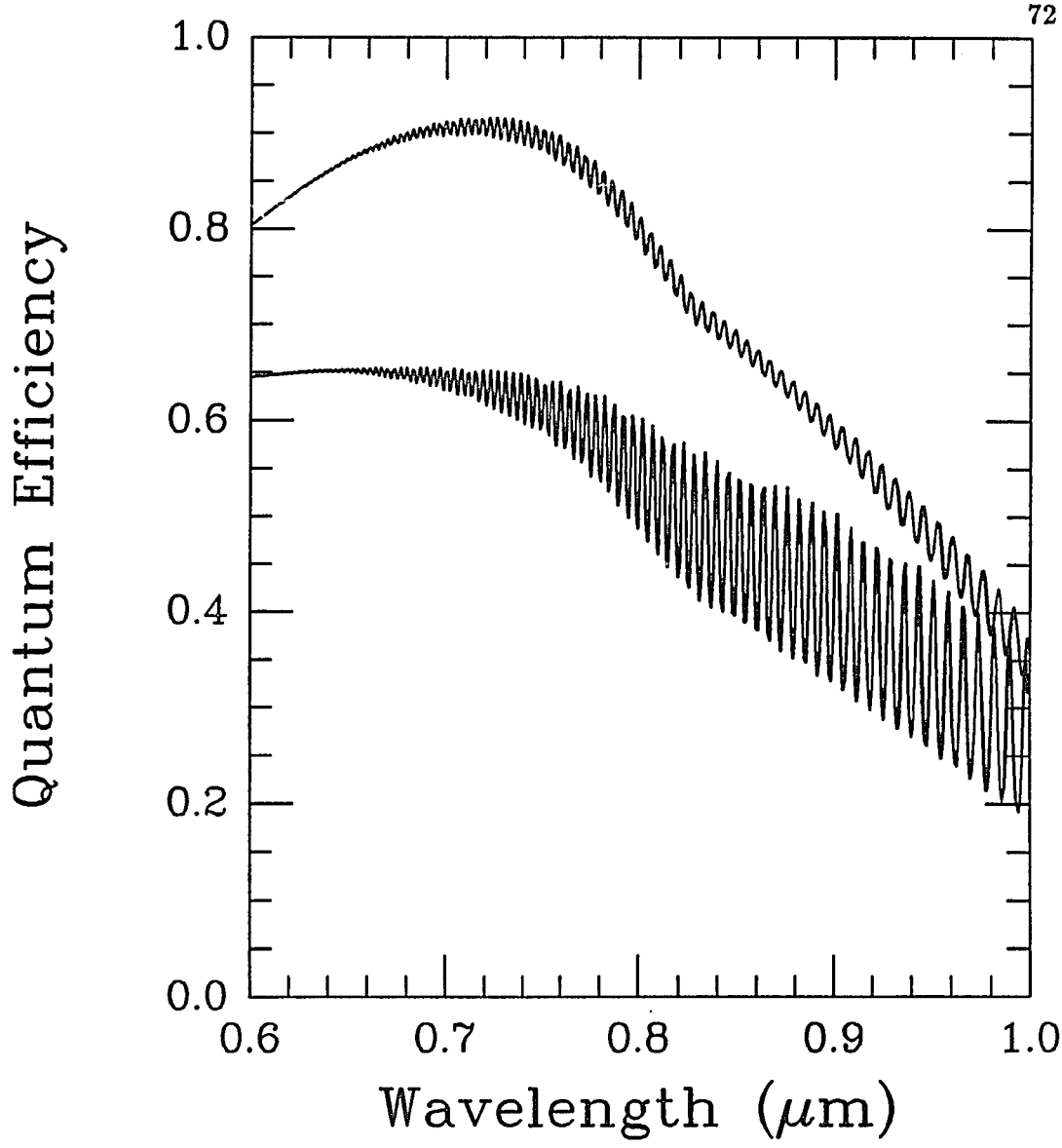

Figure 3.7. The predicted effect of a single quarter-wave AR coating on the fringing in a thinned, back illuminated CCD. The upper curve is the detector's response after application of the coating, and the lower curve before. The CCD is modeled as 15μm thick. The coating is HfO_2, optimized for 8500Å.

system protects the silicon surface. Flash gate or conductive coating charging, however, combined with proper AR coatings, will yield unprecedented external quantum efficiency throughout the UV and blue spectral region. Only the finite silicon thickness will reduce QE in the red. Applying such techniques to thicker, deep depletion devices in the future should allow these high quantum efficiencies to be obtained from the UV all the way to the silicon response limit in the near IR.

AR Coatings for Space Borne CCDs

The discussion presented here has been centered on CCD's used for ground-based astronomical observations. If sensors are to be optimized for space flight, consideration must be given to AR coatings for wavelengths below 3100Å. This is a difficult task because silicon's index of refraction decreases with decreasing wavelength from 7 at 3700Å to 0.25 at 990Å. The high index coating designs presented above for near UV and visible detectors are transparent above 2300Å, but have such high indices of refraction that they increase reflectivity and lower the CCD's QE below that of an uncoated chip for wavelengths less than about 3000Å. CCD's operating in this region should therefore be coated with only low index materials. Below 2300Å there is no known material with a low enough refractive index to AR coat a silicon detector.

CHAPTER 4

CCD BACKSIDE CHARGING

After a CCD is thinned, there is an abrupt discontinuity of the silicon crystal lattice at the backside. A thin native oxide (SiO_2) grows on this surface as the device is exposed to the ambient atmosphere. This oxide contains impurities and trapped charge which give it a net positive charge. This charge and the Si–SiO_2 interface trapped charge create a potential well near the backside which has a significant effect on free electrons within several thousand Angstoms of the interface. Any photon absorbed within this well generates a photoelectron which has only a small chance of migrating to the frontside collection wells before it is trapped and lost to recombination. Photons with $\lambda < 0.5\mu$m are most affected since the absorption depth of silicon decreases rapidly with decreasing wavelength, from more than 5000Å at $\lambda = 0.5\mu$m to less than 100Å in the UV. This backside potential well can be eliminated by applying a negative charge to the backside of the CCD to counteract the oxide charges. There are several ways of doing this — UV flooding, nitric oxide gas treatment, a Schottky barrier on the back surface, or an applied voltage very close to the backside. The UV flooding technique is routinely used on Steward's TI detectors before observing runs (Leach and Lesser 1987). Lick observatory has had excellent results with nitric oxide gas treatment of their detectors (Robinson and Osborne 1986). The Schottky barrier method is un-

der development at the Jet Propulsion Laboratory. In this chapter I present a theoretical description and initial experiments of another charging technique which offers some important advantages over current methods. First, however, the theory of backside charging is presented with some specific characteristics of existing techniques.

Charging Theory

There are two classes of charges in the CCD backside SiO_2 layer which create the backside potential well; interface trapped charge and oxide charge. The interface trapped charge density (charge per cm^2) usually dominates oxide charge in the CCD case, but the effect of both will be derived in the following discussion. The desired result is the backside voltage needed to eliminate the backside potential well and obtain maximum QE.

Interface Trapped Charge

Interface traps are defects with allowed energy levels in the Si band gap at the Si–SiO_2 interface. These traps occur both at the frontside oxide between the Si and metal/polysilicon gates and at the backside oxide which grows after thinning. The frontside traps cause the well known charge transfer problems associated with surface channel devices, while the backside traps contribute strongly to creating the backside potential with which I am now concerned. For the remainder of this discussion I will deal only with the backside oxide charges. The interface traps can exchange charge (electrons and holes) with the silicon conduction and valence bands. Traps located below the Fermi level

E_f are occupied and neutral, while those above are vacant and positively charged. It is the vacant, positively charged traps which attract photogenerated electrons to the backside and decrease blue and UV QE significantly. The actual charge trapped at the interface varies in a complex manner with backside surface potential (due to charging) as demonstrated in Figure 4.1. As the energy bands at the Si–SiO_2 interface move up (towards accumulation due to a negative backside charge), traps empty by hole capture and the amount of positive interface charge increases. In the same way, as the bands move down (toward depletion), electron capture decreases the amount of positive trapped charge. Backside charging therefore uncovers more positive charge which must be counteracted by even more negative backside charge.

In semiconductor manufacturing, the density of interface traps Q_{it} is reduced by proper thermal oxidation and annealing. Lowest trap densities are obtained when the oxide is grown in a dry O_2 environment at high temperatures (> 1000°C) and annealed after oxidation, also at high temperature. This method cannot be used for reducing the backside interface charge density because thinning takes place after frontside metalization and elevated temperatures would cause the aluminum to diffuse into the Si and SiO_2 on the frontside. Some forms of rapid, post metalization laser annealing have been used, however (Stern *et al.* 1987). The effect of such treatment on Al diffusion must be carefully studied, although the flash oxide method (described later) seems to reduce interface trapped charge densities to sufficiently low levels for backside charging. It has been repeatably demonstrated that passivating a silicon surface with an oxide impervious to water, hydrogen, sodium, etc. greatly improves the stability of Q_{it} over time (Nicollian and Brews 1982).

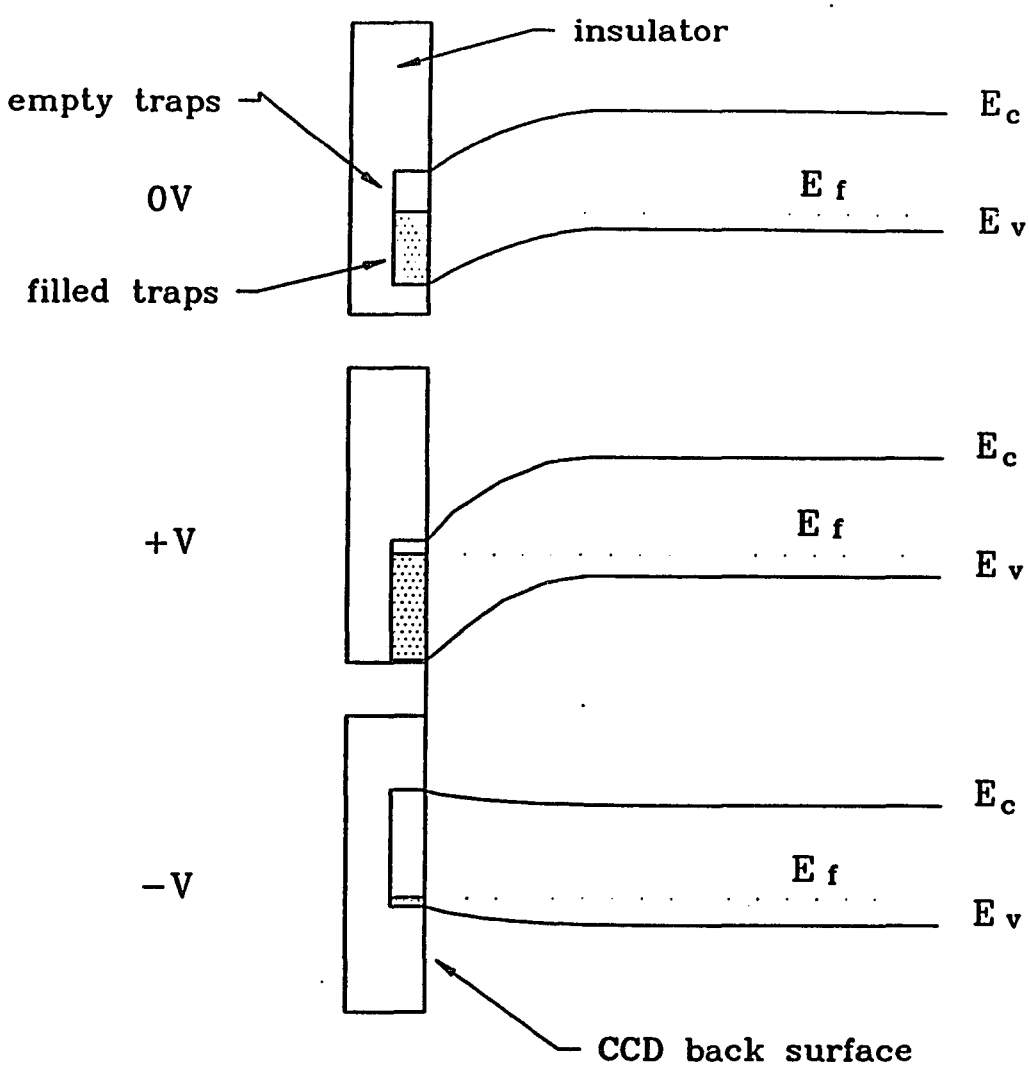

Figure 4.1. The silicon energy bands at the Si–SiO_2 interface on a CCD backside. The top figure shows the band bending when a positive backside charge is applied, while the bottom figure shows a negative bias. Filled interface traps are represented by the dots. When empty (above the Fermi level), these traps are positively charged and contribute to the backside potential well. Backside charging produces a negative bias as in the lower figure and hence additional positive trapped charge must be overcome to bend the bands upwards at the surface, creating an electric field in the Si directing photoelectrons away from the backside.

This observation, combined with the temporary and often unstable problems of existing backside charging methods, has led me to believe that passivation of the backside surface is necessary after thinning, AR coating, and backside charging. This can be done by applying a thick ($\approx 0.5\mu$m) layer of glass or other transparent insulator, or by mounting the back surface against a transparent mounting support. This aspect of mounting will be discussed further in a later section of this chapter. The purpose of the passivation is to not allow any environmental influences to affect the Si-SiO_2 interface. One advantage of the new transparent charging technique discussed later is that backside is automatically passivated by the insulator used to prevent charge leakage.

Oxide Charge

Oxide charge can be distinguished from interface trapped charge by its insensitivity to backside surface potential changes. There are two types of oxide charge; fixed and mobile. Fixed charge is created by holes or electrons injected into the oxide and trapped at trapping sites (defects in the oxide). These holes and electrons usually come from high energy processes such as cosmic rays or UV flooding. The fixed charge density is typically much smaller than the interface trapped charge density. Mobile ionic charge is caused by the diffusion of mainly alkali metal ions into the oxide from contamination sources. Sodium is the main component of this charge due to its rapid diffusion in SiO_2 and high natural abundance. Very clean processing technqiues are required to keep Na^+ levels low enough so as to not dominate interface trapped charge.

This has proven possible by following the generally accepted semiconductor manufacturing practices.

Flatband Voltage

The effect of oxide and interface charges is to produce what is termed the "flatband" voltage V_{fb}. This is the voltage which must be applied across the oxide, relative to the Si substrate, to eliminate energy band bending at the Si–SiO_2 interface. Since the oxide charges are positive, a negative charge must be applied and $V_{fb} < 0V$. Any backside charging method must at least develop a voltage V_{fb} on the backside to eliminate the backside well, and preferably a more negative voltage to create an electric field directing photoelectrons toward the frontside. I derive V_{fb} as a function of oxide charge and thickness below.

If $qn_0(x)$ is the total volume charge density from all sources in the oxide and at the Si–SiO_2 interface, Poisson's equation can be written

$$\frac{d^2\psi}{dx^2} = \frac{-q}{\epsilon_{ox}} n_0(x)$$

where $\psi(x)$ is the electric field due to all oxide charges and ϵ_{ox} is the dielectric permittivity of SiO_2 (3.4×10^{-13} F/cm). I define $x = 0$ as the oxide back surface and $x = x_0$ as the Si–SiO_2 interface. Integrating,

$$\frac{-d\psi}{dx} = \frac{q}{\epsilon_{ox}} \int_x^{x_o} n_0(x')\, dx'$$

$$\psi(0) = \frac{-q}{\epsilon_{ox}} \int_0^{x_0} dx \int_x^{x_0} n_0(x')\, dx'$$

where $\psi(0)$ is the backside voltage required to achieve the flat band condition ($\frac{d\psi}{dx}|_{x_0} = 0, \psi(x_0) = 0$). Actually, $\psi(0) = V_{fb}^{'''} - W_{ms}$ where W_{ms} is the gate–silicon work function difference, as long as electron tunneling is possible through

the oxide. Rearrange the order of integration,

$$\int_0^{x_0} dx \int_x^{x_0} n_o(x')\,dx' = \int_0^{x_0} n_o(x')\,dx' \int_0^{x} dx = \int_0^{x_0} dx' x' n_0(x')$$

to obtain

$$V_{fb} - W_{ms} = \frac{-q}{\epsilon_{ox}} \int_0^{x_0} dx' x' n_0(x').$$

If the charge centroid $\overline{x}$ is defined as

$$\overline{x} = \frac{\int_0^{x_0} x' n_0(x')\,dx'}{\int_0^{x_0} n_0(x')\,dx'}$$

and the total surface charge density Q_0 as

$$Q_0 = q \int_0^{x_0} n_0(x')\,dx'$$

then the final result is

$$V_{fb} - W_{ms} = \frac{\overline{x} Q_0}{\epsilon_{ox}} \qquad (4.1).$$

Since it is difficult to measure anything other than V_{fb}, it is the product $\overline{x}Q_0$ that is actually known, not the actual charge distribution thoughout the oxide. Detailed studies have found that, for thin oxides such as on the CCD backside, $\overline{x} = x_0$ and Q_0 can be determined from the oxide thickness and the measured flat band voltage. Thermally grown oxides have $\frac{Q_0}{q}$ ranging from 10^{11} to 10^9 cm^{-2}, depending on oxidation and annealing conditions. A bare silicon surface with no oxide has $\frac{Q_0}{q} \approx 10^{15}$ cm^{-2} due to the dangling Si bonds at the crystal surface.

Flash Oxide

Janesick (1984) finds flat band voltages for the TI 800x800 CCDs in the range -0.2 – -2V, indicating $\frac{Q_0}{q}$ is about 10^{13} cm^{-2} with a native oxide $\approx$ 30Å thick. The TI CCD backside oxides were not intentionally produced and probably took many years to grow. Janesick (1986b) has developed a technique which allows the growth of a backside oxide in a short time (several hours) with a smaller value of Q_0. This flash oxide is grown in steam at a cool enough temperature that no damage from the frontside metalization occurs. Flash oxides have actually been grown with a net negative charge under ambient conditions, indicating Q_0 is low enough that natural O_2 adsorption was able to eliminate the backside potential well. An oxide thickness of about 24Å is formed in only 2 hours of steam treatment, which would otherwise take several years to form under ambient conditions. I use a similiar recipe to grow a low temperature backside oxide after chem/mech thinning. By careful oxide growth under clean conditions, $\frac{Q_0}{q}$ can be reduced to about 10^{12} cm^{-2}, yielding $|V_{fb}| < 0.1$V for 20Å thick oxides. For thicker oxides and insulator materials such as are used in the transparent conductive coating technique, V_{fb} is larger as indicated by equation 4.1.

Existing Backside Charging Techniques

There have been many reports of successful charging efforts within the scientific community. Lind and Zalewski (1976) first reported that an ultraviolet light flood increases the UV response of silicon photodetectors. Janesick (1984) reported that a UV flood with a mercury discharge lamp produced si-

miliar results when used with a TI 800x800 CCD, as also discussed by Hlivak *et al.*. (1983), and later gave a detailed recipe for charging these devices using a zinc lamp and using [NO] gas. Robinson (1986) reported better success with [NO] charging than with a variety of other UV flooding recipes he had tried. Janesick (1986a,b) later developed the flash oxide/gate charging technique currently used at JPL and Reticon. A discussion of the distinguishing characteristics of each of these methods of backside charging is given in this section.

Ultraviolet Light Flooding

Charging by UV flooding relies on the adsorption of oxygen molecules onto the backside of the CCD with the aid of a free electron to create the O_2^- ion. This ion becomes fixed to the surface and is negatively charged. Oxygen is usually adsorbed at oxygen deficit sites on the SiO_2 surface (Morrison 1978). If there are sufficient oxygen molecules in the atmosphere near the CCD backside and sufficient free electrons in the oxide to be trapped by the adsorbed molecules, then a negative charge can be built up to eliminate the backside potential well. If an even greater negative charge is added, an electric field gradient in the Si can be produced to enhance the electron collection efficiency of the CCD. The internal quantum efficiency (percent of absorbed photons which are detected) in this condition can approach 100%.

Electrons can reach the backside of the oxide by very simple means. If light of sufficient energy illuminates the chip, photogenerated electrons will be ejected from the valence band of the silicon to the conduction band of the oxide. They are then able to migrate through the thin oxide where they

can be trapped on the back surface with adsorbed oxygen. Photons with $\lambda < 2900$Å (4.25 eV) are required for this transition. Simple gas discharge tubes of mercury, cadmium, or zinc produce radiation in suitable amounts for charging CCDs in a few minutes. These lamps emit mainly in spectral lines at 2500, 2290, and 2140Å, respectively. Due to the additional potential which must be overcome once some charge has built up on the backside, the lower energy mercury lamp is less suitable than cadmium or zinc. All three lamps have been used with successful results. The oxygen molecules needed to complete the charging can be introduced into the CCD dewar from the ambient atmosphere or from a dry oxygen supply. We have found better results are obtained when the air in the dewar is recycled several times during flooding (Leach and Lesser 1987).

Once a CCD is UV flooded, conditions must be such that the backside charge remains stable so that repeated flooding is not required. The silicon surface can discharge in a number of ways. If water vapor is allowed into the dewar, discharging will occur because H_2O is readily adsorbed on the oxide surface and donates an electron to the semiconductor, creating a positively charged H_2O^+ ion which counteracts the effect of an O_2^- ion. UV radiation is very effective at desorbing H_2O^+ ions as well as providing electrons for O_2^- trapping, allowing a net negative charge to build up. Discharge also occurs by the photoinjection of holes from the silicon to silicon dioxide valence band. This transition requires photons with $\lambda < 2500$Å (4.92 eV) and therefore occurs simultaneously with UV charging. These holes can be trapped on the backside as well as neutralize the O_2^- ions, in both cases discharging the surface. Because the mobility of holes in the oxide is significantly less than that of electrons

they do not migrate to the backside as readily and a negative net charge is achieved. To date, higher QE has been obtained with UV flooded CCDs than with any other charging technique. The major drawbacks with UV flooding are that it is not a permanent solution to the backside potential well, and its success is very dependent on backside surface properties. In particular, CCDs with p^+ substrate material left over after thinning are very difficult to UV flood and achieve maximum quantum efficiency. AR coatings cannot be applied to a CCD used with UV flooding since O_2 molecules could not reach the back surface.

Nitric Oxide Adsorption

Nitric oxide [NO] gas is believed to be adsorbed dissociatively on the silicon surface such that N and O atoms bond separately to adsorption sites. The energy of the resulting electron traps is low enough (below the Fermi level) that electrons which tunnel through the thin oxide layer can become trapped and no UV flooding is required. The [NO] gas must only be introduced near the CCD backside for charging to occur. This implies that the energy levels of the [NO] electron traps are below the Fermi level, while the O_2 traps are above. The same conditions as described under UV flooding are required to maintain the fully charged condition after [NO] charging. Lick Observatory has maintained [NO] charged TI 800x800 CCDs for many months without any noticable loss in quantum efficiency (Robinson and Osborne 1986). The major problem with this method is the high toxicity of nitric oxide – a few ppm inhaled over a period of a few hours can be fatal. [NO] has also been found to be corrosive to some dewar materials, particularly copper. As with UV

flooding, [NO] charging is not a permanent solution to the backside potential problem and its effect is highly dependent on backside surface characteristics. AR coatings also cannot be applied to [NO] charged sensors because of the need for gas adsorption on the back surface.

The Flash Gate

Electron tunneling can occur through a thin (< 50Å) oxide on the CCD backside if a metal is deposited on the outer oxide surface. Depending on the work function (the energy required to move an electron from the Fermi level to the vacuum level) of the Si and metal, electrons can flow either from the Si to the metal or *vice versa.* When the work function of the metal is larger than that of Si, electrons flow to the metal and a negative backside charge builds up. If this charge is large enough, the backside potential well is eliminated.

The net backside charge obtained from this flash gate system is determined by the interface trapped charge density, oxide charge density, and Si work function at the back surface. The work function is dependent on the silicon Fermi level (and hence the doping concentration) and is larger for p^+ Si than p Si. The only common materials with sufficiently high work functions are platinum, gold, and nickel; of these Pt is best. In practice less than 10Å of Pt are needed to fully charge a CCD after a high quality flash oxide is grown. This is so thin (approximately one monolayer) that the Pt has a fairly small optical effect on CCD operation.

The major difficulty with the flash gate charging method is that is very sensitive to backside surface conditions and proper oxide growth. If the oxide and interface contain too many positive charges, enough electrons cannot be

transferred to eliminate the backside well. Any p^+ material can especially effect the charging properties since W_{ms} is significantly reduced. The great advantage of the flash method is that once charged, the backside well is permanently eliminated. There are some environmental effects which can discharge the CCD, and more research is needed to improve the QE stability of the flash gated CCD. If this problem is associated with diffusion of H through the Pt flash gate, it might be solved with backside passivation. AR coatings can be applied after flash gate deposition since adsorption of ambient molecules is not necessary.

Transparent Conductive Coating Charging

Due to the astronomer's need for a CCD with maximum QE and very stable characteristics, I will present a theoretical developed of another method of backside charging that allows AR coatings to be applied and can be applied to a wide variety of CCDs. This transparent conductive coating (TCC) technique consists of applying a negative voltage from an external power supply to a transparent conductive thin film deposited directly on (or near) the CCD backside. In effect, a metal-insulator-silicon (MIS) capacitor is formed directly on the backside. The electric field so generated will eliminate the intrinsic backside potential well in the same way that a negative charge build up does with UV flooding, [NO] adsorption, or the flash gate. The applied voltage can be varied to give maximum QE for devices with different backside characteristics. In particular, a higher Si-SiO_2 interface potential can be obtained than with other charging methods. This results in more uniform QE across the device since backside characteristics such as residual p^+ material

and thickness variations will not effect QE (in the blue and UV). A large enough interface potential generated from backside charging will compensate for potential well variations caused by surface impurities. A voltage controlled backside charge is insensitive to work functions or environmental conditions. The CCD backside becomes passivated against environmental conditions and the conducting gate is too distant from the Si-SiO_2 interface for electron tunneling to occur. Since there is no reliance of gas adsorption with this charging method, AR coating can be applied as discussed in Chapter 3. The major difficulty is the actual deposition of a suitable sufficiently transparent conductive coating and its required insulator.

The backside of a CCD using the TCC charging method is a simple metal-insulator-semiconductor capacitor. The gate voltage applied to the conductive film brings about a change in the energy bands in the silicon. Equation 4.1 relates the Si–SiO_2 interface potential to this gate voltage in terms of the oxide (insulator) thickness and dielectric permittivity. The most stringent requirement for the operation of such a capacitor is that the current flow through the insulator be less than the dark current of the CCD (2 e^-/pixel/hour at $-140°C$). During normal semiconductor processing, insulators (SiO_2) are grown at $\approx 1000°C$, typically 1000Å thick. They have no pin-holes and a resistivity of near $10^{19}\Omega$ cm. As discussed previously, thermal oxides cannot be grown on the CCD backside so other means of producing an insulator must be found. The ideal system uses an AR coating to increase QE as well as act as the TCC insulator. This is possible if AR coatings can be deposited without any pin-holes through which charge can leak. My experiments have shown this to be nearly impossible for the thin coatings required for silicon AR coatings,

especially since they must be deposited on the CCD cold and therefore do not grow well after initial nucleation. Fortunately the mounting technique I have choosen to keep the CCD flat and stable also allows the TCC to be feasible. The cement used to bond the CCD to the transparent substrate is electrically insulating and at least one micron thick. It has sufficient insulating properties to keep charge from leaking into the CCD when the conductive coating is deposited on the substrate instead of the CCD itself. Unfortunately, this same thickness decreases the capacitance of the Si–insulator–coating system considerably, and large backside voltages are required ($|V_g| > 50V$, see eq. 4.1).

Metallic Coatings

The requirements of the TCC material for backside charging is high optical transparency from the atmospheric limit to the silicon bandgap edge with sufficient conductivity to apply a uniform charge across the entire active CCD area. The most obvious choice for the TCC material is a thin metallic film. Quite high sheet resistivities can be tolerated for this film since the field generated is static. In fact, the actual requirement is simply that the film be electrically continuous over its entire surface. Many such films have been produced by other researchers with mean thicknesses less than 10Å (Hoffmann and Fischer 1975, Hoffmann *et al.* 1985). Figure 4.2 shows the theoretical transmission of several thin metallic films. Each of these can easily be applied to the CCD backside by thermal evaporation, requiring the substrate to be only at room temperature. Silver and copper coatings not protected from the atmosphere after deposition will quickly tarnish due to oxidation. Silver is an

excellent material for these films provided an overcoating is used for protect from corrosion. A multi-layer Ar coating with the Ag film between layers is ideal for this purpose if the coatings could be deposited with sufficient insulating properties. When deposited on the glass mounting substrate the cement keeps the silver from oxidizing. The entire system is passivated from environmental effects by the substrate and cement and should therefore remain very stable over time. My experiments have determined that 20Å thick, vacuum deposited metallic films of silver do in fact have high transmission and are electrically conductive, as shown in Figure 4.3. Thinner layers are not fully conductive, since the films grow from nucleation centers on the substrate surface and these would not yet be fully contacted to each other.

Metal Oxide Coatings

Due to the low optical transparency of most of the thin metal films, I have investigated TCC films made from more transparent materials such as metal oxides. These films, such as tin oxide and indium tin oxide (ITO) are optically transparent over most of the spectrum of interest for astronomical CCD observations. They are electrical conductive, but can cannot be applied directly to the CCD surface. High transmission can only be obtained with these films by heating the substrate they are to deposited on to more than 400°C, which would damage the CCD. However, using a backside glass support substrate to maintain surface flatness after thinning does allow for metal oxide film deposition. When bump bonding is developed such that a backside substrate is no longer used, metal oxide films could not be used.

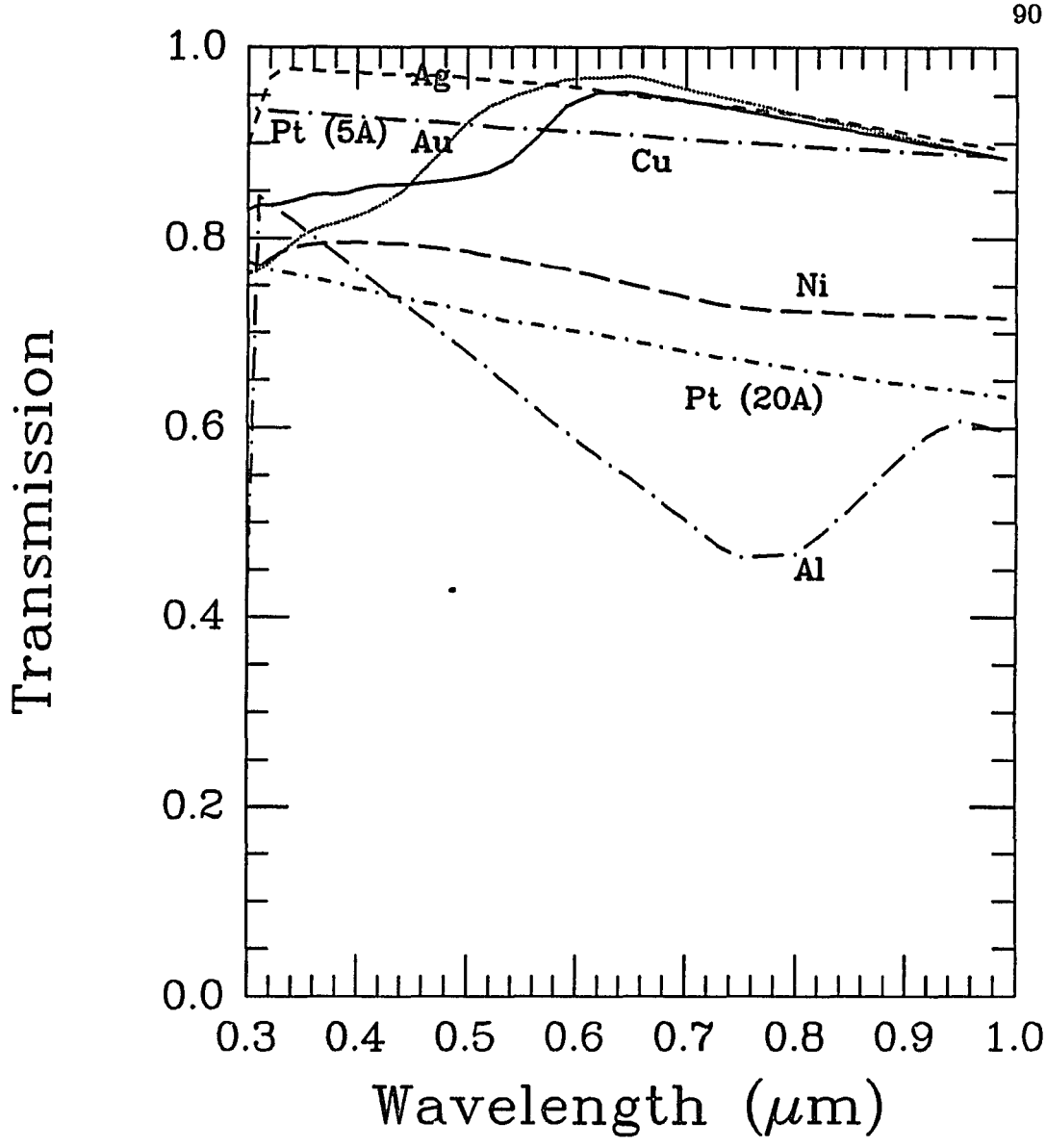

Figure 4.2. The transmission through several thin metallic films. All films are 20Å thick except for one 5Å Pt film shown for comparision. The flash gate (Schottky barrier) method of charging uses a 5 – 10Å Pt film. It is interesting to note that the conductive 20Å Ag film has higher transmission than the flash gate. The actual transmission of these films on the CCD backside will be a few percent higher due to refractive index matching to the backside insulator and overcoating.

The metal oxide thin film coating I have experimented with is indium tin oxide (ITO). This material has been used extensively in the past for heaters on glass windows and a vast amount of literature is available on its properties and application techniques. I have experimented with thermal evaporation of ITO onto glass. Sufficient conductivity can be obtained in films $\approx$ 300Å thick (Vossen 1977, Mizuhashi 1980). Figure 4.3 shows a comparison of a 20Å thick Ag film and a 450Å thick ITO film which I deposited on quartz microscope slides. The ITO coating has excellent tranmission in the visible and is extremely durable. The high UV absorption, however, makes it less desirable for use as a TCC since the goal is to obtain high blue and UV quantum efficiency. Thinner ITO coatings will be pursued in the future to take advantage of ITO's other excellent characteristics.

Discussion

The major difficulty with charging CCD's is that there is a great deal of variability among devices. Janesick's work with a large number of sensors has shown that one factor which heavily influences the ability to charge a CCD is the amount of heavily doped p^+ silicon left on the backside after thinning. The distribution of this p^+ silicon is usually non-uniform across the chip's surface and causes non-uniform response to backside charging, due to its different conductivity. In addition, the higher doping of the p^+ material means the minority carrier lifetime is shorter than in the p material, so photogenerated electrons have a higher probability of recombining before being detected. All charging techniques therefore require precise thinning which can remove all

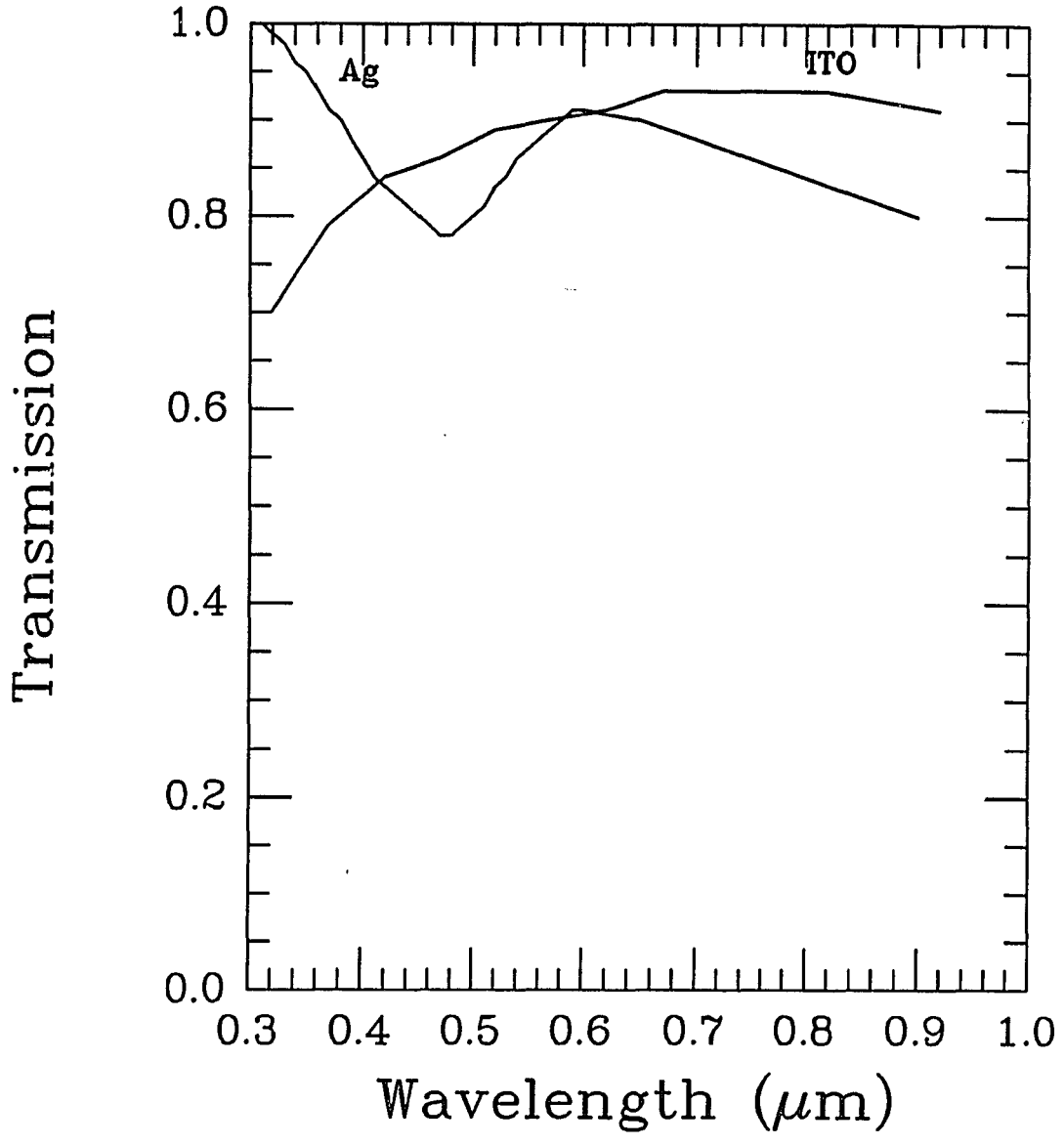

Figure 4.3 The measured transmission of two thin, conductive, thermally evaporated coatings. The ITO and Ag films are 450Å and 20Å thick, respectively. The Ag shows superior UV transmission, and is an excellent material for CCD TCC charging. The ITO film has better visible and near-IR transmission but is unacceptable in the UV. It is possible to deposit thinner ITO films which should have better UV transmission, but these have not yet been successfully made at our vacuum facility. As discussed in the text, the ITO film must be deposited on a hot substrate, and therefore cannot be applied directly to a CCD backside.

p^+ silicon from the CCD backside. Conductive coating charging relaxes this constraint somewhat when a high enough backside charge can be applied to reduce the p^+ material effects. The chem/mech thinning method affords the control necessary to meet this thinning requirement as long as the p^+ diffusion region does not extend too close to the CCD frontside. In general this diffusion region is limited to within 2μm of the epitaxial interface. As CCD's are built with thicker epitaxial layers, it will be much easier to remove all p^+ material from the CCD backside and charging will allow even more uniform quantum efficiency to be obtained. The ideal astronomical CCD imager requires a thick epitaxial layer, uniform thinning which removes all substrate Si, and AR coatings combined with a metal flash gate or TTC to increase quantum efficiency. Over this system a passivation material can help to reduce environmentally induced QE instabilities if the AR coating is not sufficient for this purpose. Such a device offers QE in excess of 80% from the atmospheric cutoff to well into the near IR. When combined with a stable mounting package such as a backside transparent support or frontside bump bonding substrate, many of the current observational problems of astronomical CCDs will be eliminated. The remaining difficulty is the manufacture of CCDs with high quality electronic properties. Although this is certainly a difficult problem, a number of such devices have already been produced and more will certainly be available in the future.

CHAPTER 5

CCD MOSAICS

With the development of the optimzation techniques presented in the previous chapters, and the availability of commercially produced CCDs to which they can be applied, the major drawback of CCDs as astronomical detectors is their small physical size. While large photographic plates for telescopes are well over 1500 cm^2, the largest CCD's in current use are only 1 cm^2. Even the Tektronix 2048x2048 pixel CCD which has been expected to be commercially available during the last few years is only 31 cm^2. A typical Ritchey-Cretian telescope's focal plane is well over 500 cm^2, and the eight and ten meter class telescopes of the next decade will have even larger focal planes (Angel 1984, Hill 1987). It is clear that some form of efficient large area CCD detector or detector system must be developed for optimal use of large telescopes.

There are several possible methods of using CCDs in large area light detection systems. These include producing large individual devices, building a focal plane mosaic of many smaller devices butted closely together, or optically constructing a mosaic using fiber optics or beam splitters. In this chapter I present a focal plane mosaic design using current generation CCDs which are butted together on a single support. The optimization techniques described in the previous chapters are intrinsically a part of this mosaic development, and in fact developing a CCD mosaic was the initial driving force for this dissertation.

Since CCDs of the quality required for astronomical observations have not been available for the contruction of a mosaic, work has been focused on individual devices. When single high quality CCDs have been fully characterized and successfully used for astronomical observations after chem/mech thinning, AR coating, and backside charging, mosaic construction will be appropriate. Before describing the details of my design for a focal plane mosaic, I will discuss some aspects of other large area detector systems which might be used for astronomical observations.

Large Area Detector Systems

Single Detectors

The most obvious method of obtaining a large detecting area is to use large area, individual detectors. The largest solid state detectors yet produced are the Tektronix 2048x2048 pixel (5.13x5.13 cm) CCDs (Blouke *et al.* 1987). While these devices represent a major advance in solid state detector area, their commercial release has been delayed by several years due to problems associated with charge transfer traps (Blouke *et al.* 1988). These traps exist in devices from other manufacturers as well, but have been very severe in the Tektronix devices. This is not necessarily due to their large size since smaller 512x512 pixel Tektronix devices exhibit the same problems. The very large physical area does, however, strongly influence the yield of acceptable devices since there is a higher probability that a fatal manufacturing defect will occur in a larger detector. The raw silicon crystal itself must be of extremely high

purity to allow an adaquate manufacturing yield. These difficulties and the very large expense required to solve them have made the production of large area single CCDs a difficult task. The successful development of such devices rests almost entirely with the manufacturers unless astronomers and other scientists can commit very large funds towards such projects.

The operational aspect of individual large area detectors is less suitable for astronomical use than a mosaic of smaller devices for two fundamental reasons. First, single devices take a very long time to read out the entire image, especially considering that the low noise requirement of astronomical observations requires long signal integration times. The large Tektronix CCDs now takes several minutes to read (Monet 1987). A separate but associated problem is the charge transfer inefficiency of shifting charge through a very large number of pixels. Even with a charge transfer efficiency (CTE) of 0.99995 per phase, 46% of the charge in the pixel furthest from the amplifier in a 2048x2048 CCD is lost. Both of these problems may be lessened by using multiple amplifiers on a single device, although the complexity of the controller electronics for such a device would be nearly identical to a mosaic controller.

Optically Multiplexed Detectors

Rather than rely on single large area detectors, several groups have taken advantage of large focal planes by simulating large detectors using a multiplexing technique which splits the focal plane into smaller regions. This multiplexing can be done with a boule of coherently bundled fiber optics (Gorham *et al.* 1982, Hobbs *et al.* 1983, Williams and Weistrop 1983) or an optical beam splitter (Lockhart 1982, Gunn *et al.* 1987). These methods

have met with considerable success, but do not allow for expansion to the focal plane dimensions required of future large telescopes. For this reason, I have chosen to develop methods to produce CCDs mosaics directly in the focal plane, requiring no intervening optics.

Focal Plane Mosaics

A focal plane mosaic of very high quality, astronomical grade CCDs can be constructed using the optimzation techniques presented in the previous chapters of this dissertation. The CCDs themselves can be purchased from whichever CCD manufacture is currently producing the devices with the best electrical properties such as low noise, dark current, and good CTE. At the time of this writing this would probably be Thompson-CSF devices, although Ford, Reticon, and Tektronix may be selling competitive detectors soon. Before discussing how the optimization techniques specifically relate to mosaic construction, I will briefly discuss a type of CCD which would make mosaics more attractive to many observers – the buttable CCD.

Buttable CCDs

A buttable CCD is constructed for use in mosaics by locating all wire bonding pads on one or two edges of the device and allowing the active imaging area to extend as close as possible to the other edges. In this way it is possible to obtain gaps between two devices in a mosaic as small as ten pixels (typically less than 300μm). Buttable devices have been used for many years for military applications (Ibrahim *et al.* 1978, Burke *et al.* 1980), and

have recently been developed for scientific applications by Thompson-CSF. I have not based my CCD mosaic designs on buttable devices simply because the development of any new CCD has traditionally been a very long, expensive, and difficult task. If buttable CCDs of sufficient quality are available when devices for a mosaic are to be purchased, they can be used advantageously to achieve smaller image gaps. The same basic mosaic construction methods will apply. It is worth noting that buttable devices requires thinning over their entire surface since the pixels extend nearly to the device edges. The chemical/mechanical thinning method presented in Chapter 2 is well suited to thin in this manner, but traditional acid etching usually thins the detector's central region only to avoid etching device edges.

Mosaic Mounting

There are two feasible methods of mounting CCDs for operation in a back illuminated focal plane mosaic. The devices can be mounted with their back surface bonded to a transparent substrate, or they can be bump bonded to a silicon substrate on their front side. The bump bonding technique is the most feasible method of making very large area mosaics (more than about four devices) and will be the main subject of discussion here. The transparent substrate method, however, is considerably simpler and requires no untried technology such as bump bonding of CCDs. It can be used for small mosaics and will most likely be used for the first mosaics to be built, including the spectroscopic mosaic design presented in a later section. I will therefore discuss, as appropriate, differences in mosaic construction for these two mounting schemes.

A mosaic of thinned CCDs can be made by using the bump bonding technique in which each device is bonded to a single silicon substrate. Silicon substrates are now routinely produced up to six inches in diameter (for large integrated circuit wafers), on which over 100 conventional CCDs could be mounted. It is advantagous, however, to use smaller substrates when constructing large mosaics to minimize device loss if a substrate breaks or otherwise fails. From my experience with packaging (and unpackaging) CCDs, it is not possible to routinely remove a working CCD from a package after it has been mounted and bonded. The economic advantage of a mosaic in terms of device failure should not be overlooked. A single large area CCD may cost many tens of thousands of dollars. If it breaks, or its amplifier is destroyed due to static electricity or other mishap, then the entire device is lost. If a single device in a mosaic is destroyed, the other detectors can be operated with only a loss in spatial coverage. However, in a mosaic the substrate to which the devices are bonded may fail, possibly resulting in the destruction of all devices on that substrate. For this reason, there is a maximum number of devices which should safely be mounted on a single substrate. The first generation mosaics will be three or four devices – easily mounted on a single silicon substrate.

It is also possible to mount CCDs with their back surface against a large glass or sapphire substrate. I have successfully used this technique with individual devices (see Chapter 2) and its extension to multiple devices is certainly straightforward. Each CCD is thinned on a thinning support, the backside is treated with a flash oxide, AR coating, and charging material, and then is transferred to the common transparent mounting substrate of the mosaic. The major difficulty with this technique is the possibility of breaking or

warping the thin silicon during transfer. A small mosaic can be built using this technique as soon as controller electronics and sufficiently high quality devices are available. As previously mentioned, I do not believe this is a realistic approach for large scale mosaics due mainly to the electrical interconnection problems.

Electrical Connections

Mounting CCDs butted together does not readily allow for conventional wire bonding as with a single device in single package. Without the use of bump bonding, wire bonds must be made from each bonding pad on each CCD to a bonding area on a interconnection printed circuit board. This is impractical for a large number of devices due to the complexity of the required bonding. Bump bonding allows all electrical connections to be made using photoresist processes on the silicon substrate, a technique well suited for this task. Figure 5.1 shows a schematic representation of a three CCD linear mosaic which could be produced on a transparent substrate using conventional wire bonding. Even for this small number of devices the mounting/bonding can be seen to be rather cumbersome, although certainly feasible. Larger mosaics should certainly take advantage of semiconductor industry advances in packaging such as bump bonding.

After the CCDs are bump bonded to a substrate, electrical contact must be made from the many substrate connections ($>$ 100 for even a small mosaic) to connectors leading to the controller electronics. With bump bonded substrates these connections can be made simply using conventional wire bondings from bonding pads on the periphery of the silicon substrate to a printed

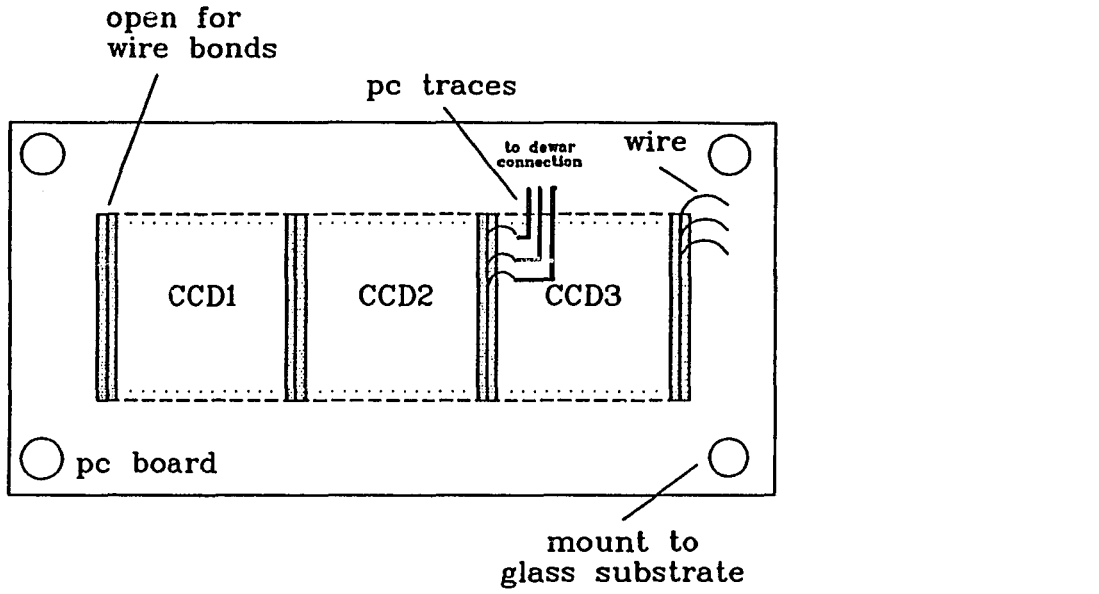

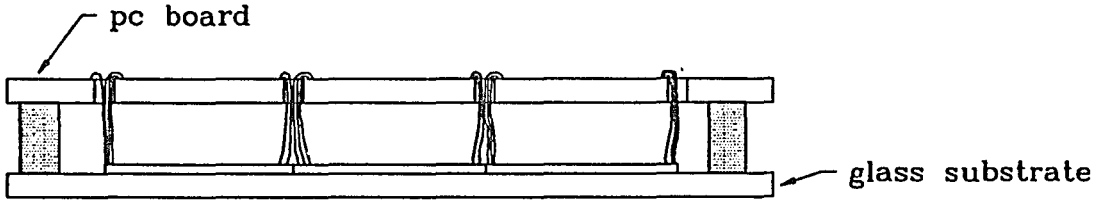

Figure 5.1. A schematic representation of a three CCD mosaic mounted on a transparent support. Wire bonds are made through slots in a PC board (or other support) to each device bonding pad. See text for details. This is an example of a simple mosaic for use with the MMT Blue Channel Spectrograph.

circuit board with matching pads and electrical traces leading to connector sockets. This step is necessary since wire connectors cannot be used directly on a silicon substrate. Figure 5.2 shows a schematic representaion of such a bump bonded mosaic incorporating these ideas. The technology to implement all these aspects of mosaic packaging exist today and are in routine use by the semiconductor industry. Only the actual bump bonding of CCDs has not been demonstrated, but is expected to present little problem since many other devices have been bonded in the same manner as required for these mosaics.

If a transparent substrate is used instead of bump bonding for a small scale mosaic, wire bonding would be used directly to a printed circuit board as discusssed above. The wire connections to the controller electronics would then be made directly to this board, and no intermediate steps are necessary. The difference in the PC boards would be that the wire bonding pads must match the CCDs' bonding pads rather than arranged in a more convenient pattern around the periphery of the board. Actual wire bonding would be much more difficult and a special bonding machine may be necessary to reach through the PC board to make the connection to each CCD, as in Figure 5.1.

Cooling

Each CCD in a mosaic must be operated at cryogenic temperatures ($\approx -120°C$) to reduce dark current to acceptable levels (several electrons per pixel per hour). The entire mosaic substrate must therefore be cooled using liquid nitrogen. For a bump bonded substrate this is accomplished using a cold finger in contact with an LN_2 reservoir and the substrate backside (opposite to where the devices have been bonded). Temperature stability can be main-

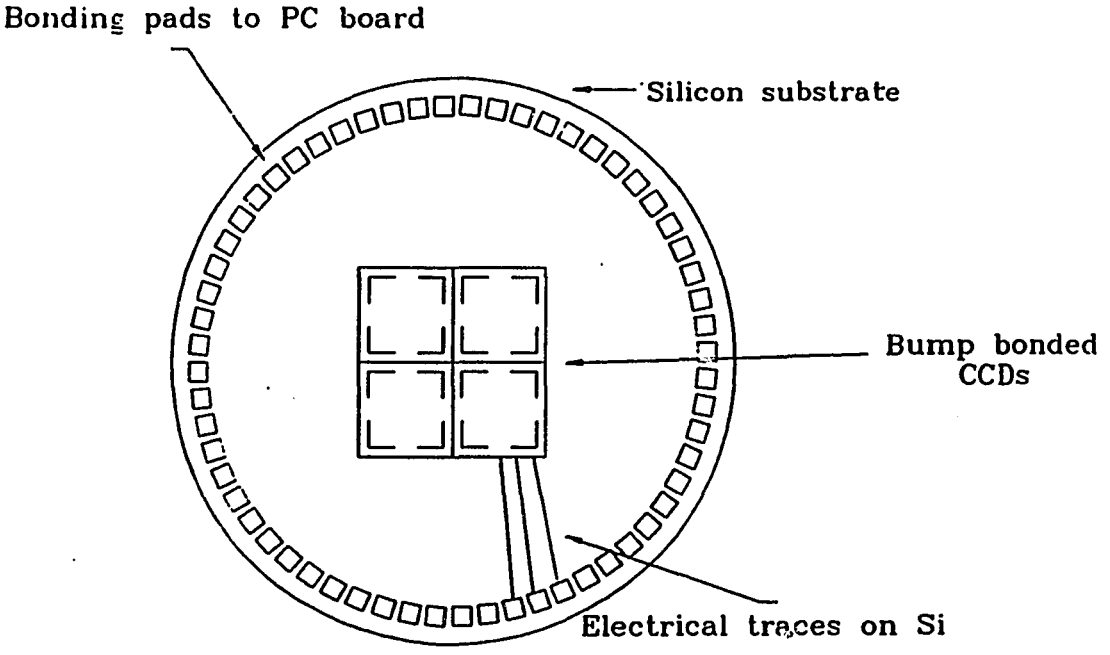

Figure 5.2. A schematic representation of a four CCD bump bonded mosaic. The backside of the CCDs is shown, with the dashed lines indicating the borders of the active and nonactive detector area. Only some of the traces from bump bonding pads to wire bonding pads are shown for clearity. The wire bonding pads and traces are aluminum, deposited using standard photoresist techniques.

tained by a copper block also in contact with the substrate backside to which a controlled heater element is attached. The major difficulty is minimizing the heat loss of the large area substrate, especially considering the large radiative loss through the dewar window. This window must, of course, be much larger than conventional windows to illuminate all devices in the mosaic. This additional heat loss will decreased the hold time of the dewar, which can be offset by using a larger LN_2 reservoir. The entire dewar will be fairly large to allow for the mosaic and any preamplifiers required (one for each CCD), and so a larger reservoir should present no problem.

Physical Device Registration

Critical registration or alignment of each CCD in the mosaic is not a major problem because of the observing techniques which will be used to operate the mosaic. With all observations, the final image must undergo a considerable amount of post data processing steps, such as flat field calibration, bias level correction, and, usually, multiple exposure summation. When these steps are carried out, it is a simple matter to register all subimages onto a single final image plane which has a constant spatial scale. Multiple exposure of the same field always undergo this transformation even when single devices are used. The alignment of each device is not critical since any spatial information derived will be based on pixel location in each subimage and the absolute offset of each device with respect to the others. The relative position of each device in the mosaic with respect to all others must be known for each exposure. Hopefully this will not change throughout the night, but one additional calibration step not currently taken with single detectors must be introduced. The calibration

procedure for determining individual detector positions independent of any flexure or thermal effects could consist of an exposure of an artificial grid of point sources taken in the same manner as conventional flat field calibrations. The mechanism to make such expoures must be included in any mosaic design.

Mosaic Observing Methods

The use of mosaics for spectroscopic observations does not allow a large variablity in design and will be discussed with a detailed design for a specfic spectrograph camera in a later section. There are several techniques, however, which can be used for direct imaging with a CCD mosaic, each well suited for different goals. If exposures of known fields are to be made in which image seams are acceptable if suitably placed, single exposures can be made for each field. The resultant image will contain gaps between the images from each CCD. These gaps will be small (less than $\approx$ 20 pixels) if buttable CCDs are used, or larger ($\approx$ 100 pixels) with non-buttable devices. A spatially continuous image cannot be produced from such an observation. For many purposes this is acceptable, as in photometry of a large number of objects. However, if an image of an entire region of sky is desired, then multiple exposures are necessary to "fill in the gaps". With such multiple exposures, a final seamless image can be created by shifting the center of observation of each exposure. Combining the subimages will be done as a post observation image data reduction step. It should be noted that the signal-to-noise ratio in the final image will vary across the image depending on the exposure time each pixel in the final image received. Two exposures of half the total integration

time desired are necessary at a minimum, with the SNR of those regions observed only once reduced by aproximately $\sqrt{2}$ for low readout noise devices and sufficiently long exposures. Signal-to-noise will be more uniform if many exposures are taken, each image shifted slighty from the others, although a penalty will be paid for read noise and increased data storage requirements. Many exposures will also reduce problems associated with flat field calibration since each part of the sky will be observed by different pixels in the mosaic (*e.g.* Tyson 1986).

Another approach to direct imaging with a CCD mosaic takes advantage of the drift scan or time-delay and integrate (TDI) observing method. With drift scanning, the CCD is clocked in the vertical direction at the same rate as the sky is drifted across the detector. Scanning across the sky can be accomplished by shifting the detector or, more easily, by allowing the telescope to track at a non-siderial rate or by not moving the telescope at all. This method has been used successfully with single devices (Mackay 1982) and is now routinely used in the CCD/Transit Instrument (CTI) at Steward. CTI uses two RCA CCDs mounted in a single dewar in two conventional packages (McGraw *et al.* 1986). One advantage of drift scanning a CCD mosaic is that seamless images can be produced using a linear arrangement of devices. This is accomplished by staggering the CCDs such that the imaging area of each device overlaps the imaging area of its nearest neighbors, as shown in Figure 5.3. The final image will have the dimension of the number of pixels in the mosaic perpendicular to the drift direction by an arbitrary length determined by the exposure time in the drift direction. Integration time for each pixel in the final image is determined by the time taken to drift an element of sky across

a single detector in the mosaic. This can be varied by the tracking rate of the telescope (which requires varying the clocking rate of the CCDs). Because the CCDs would be physically staggered in their mounting, the exposure time across the image will not be constant near the "bottom" edge of the final image. This part of the image will not yet have traversed the entire width of each CCD when the exposure is terminated. The fraction of the final image with this non-uniform integration time will decrease with increased exposure time.

The drift scan technique also offers the advantage of improved flat field uniformity since each element of sky is observed by all pixels in one column of the CCD. This essential averages the response of each column. Only column to column average uniformity responses must be calibrated, and by using the techniques presented in the previous chapters these variations will be very small.

CCD Selection for Mosaic Detectors

The selection of CCDs for single detector cameras is usually not difficult when sufficient quality devices are available. This problem requires careful consideration for mosaics, however, because of the mounting method used. Individual devices will be bump bonded to a silicon substrate (or mounted on glass), and then thinned using the chem/mech process. Once bonded, they cannot be replaced if they are found to be defective. Bump bonding can only be done once in any device location in the mosaic due to the processing requirements for producing the substrate bumping pads. Only devices known to be of acceptable quality should therefore be initally bonded. These devices

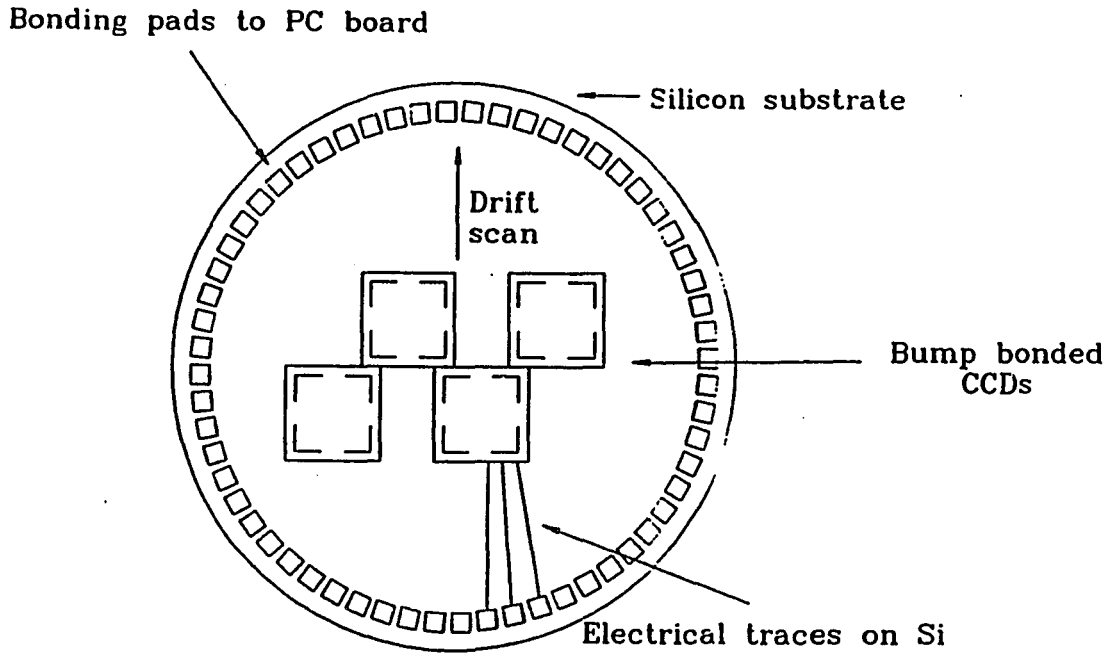

Figure 5.3. A schematic representation of a four CCD bump bonded mosaic for drift-scan observations. See figure 5.2 for other details.

must be initially tested at cryogenic temperature since many CCDs operate at room temperature but not when cooled. Currently, the only way to test CCDs when cooled is to operate them in a dewar after full packaging. Wafer probing stations used by CCD manufacturers are now capable of testing at room temperatures only. It is therefore necessary to build a cryogenic test station to test the CCDs to be used in the mosaic. This facility must cool individual devices and test their electrical properties such as read noise, linearity, and charge transfer efficiency. The CCDs would be tested in the front illuminated mode since they would not yet be thinned. Quantum efficiency measurements are not needed as QE will depend entirely on the device thickness and backside properties after thinning. The CCDs must be removed from the facilty after testing and bump bonded to the mosaic substrate. The test mounting is therefore temporary and must not destroy the bonding pads or damage the silicon when the CCD is removed. To my knowledge, this capability does not currently exist and must be designed and built before constructing a mosaic. It should be possible to build such a test facility using conventional dewars and wire bonds which can be pulled up without damaging the bonding pads. Another possibility is to use probes to contact the CCD bonding pads as in wafer probe stations. This method will cause less damage to the CCD and can be easily implemented to test many devices. The disadvantage is the increased complexity of the test dewar. For small scale mosaics, testing in conventional dewars with wire bonding into temporary (non-expoxied) packages will be feasible.

Mosaic Controller Requirements

Although the successful operation of a CCD mosaic depends strongly on the design and implementation of the controller electronics used for its operation, this aspect is beyond the scope of this dissertation. I will discuss, however, some of the important requirements which any mosaic controller must meet. The implementation of these requirements can best be met by careful design using the rapidly advancing electronic technology available at the time of the controller construction.

The single most important aspect of controller design which has direct observational influence is the parallel readout of each CCD in the mosaic. If all devices were to be read out in a serial fashion, the observing time lost during readout would be prohibitively large. A single 512x512 pixel device now takes about 20 seconds, at a pixel rate of 20k pixels/sec. A mosaic of ten such devices would take over 3 minutes, a substantial wait for the observer and a significant loss of observing time, especially with short exposures. With only a few devices this lost time is less important, although such mosaics should also act as prototypes for future large area mosaics and therefore implement as many similar features as are practical. Current high speed computers and DMA controllers now make parallel readout a practical approach. A mosaic operated in the drift scan mode will not pay a penalty for lost observing time with serial operation as long as all CCDs can be read in the time required for a single vertical clocking.

Although parallel readout is important for a mosaic, each device will require different operating parameters for optimal operation. As an example,

the gate and amplifier voltages will be different for each device, even though the clock waveforms may be the same. One simple way of implementing this is to use common clock waveforms, but with separate clock drivers for each device. Only a single timing generator is required for the entire mosaic, with separate clock driver and video processor cards for each CCD. A multiplexing scheme could be derived to allow more than one CCD to use the same analog-to-digital converter, depending on its speed and the number of CCDs in the mosaic. This general scheme can be expanded by operating large CCD mosaics as groups of smaller mosaics, each multiplexed and operated in parallel.

When large numbers of CCDs are to be used in mosaics, automated characterization of their operating parameters becomes important. Computer controlled clock voltages for each CCD, implemented with digital-to-analog converters, is an excellent method of accomplishing this goal. Not only can a computer program be used to find the optimal settings for each CCD, but more compex forms of clocking are easily achieved such as ramping and separate voltages for integrating, readout, and flushing. A prototype controller using many of these design features has been designed by Leach at Steward and is currently under construction.

Data Storage and Analysis Requirements

The storage and analysis of data obtained with a large area CCD mosaic must be a serious consideration of any mosaic design. A ten CCD mosaic, quite small compared to what is needed to populate an eight meter telescope focal plane, can produce hundreds of megabytes of observational and calibration data each night. It is important to reduce this vast quantity of data to

more reasonable values as soon as possible, and certainly before leaving the observatory. It is a necessity, therefore, to have near real-time data reduction capabilities which can at a minimum make the required instrumental corrections such as flat field and bias calibration. Construction of single, seamless images when appropriate should also be done at the observatory site since all required data is available and easily automated. With this technique, the observer need only keep instrumentally corrected images on permanent storage medium. Storage media of higher density than the 2400 foot 6250 bpi tape reels would certainly be desired. Fortunately, the market for large capacity digital storage media is rapidly advancing and devices such as optical disks will probably be available when required for large mosaics.

The actual analysis of the large amounts of data obtained with a CCD mosaic will also present a problem to the observer. Faster computers will significantly speed up such work, but changes in analysis techniques may also be required. Automatic search and classification alogithms may be necessary to sift through the raw data. Such techniques are discussed in connection with the CTI data analysis (Cawson *et al.* 1986) and much about the operation and reduction of large quantities of data can be learned from the continual data stream obtained with this instrument.

A Spectrographic Mosaic for the MMT Spectrograph

An application of a small scale CCD mosaic to demonstrate the techniques discussed here as well as provide very high quality astronomical data is a new detector for the Multiple Mirror Telescope (MMT) Blue Channel

Spectrograph. This instrument currently uses a dual intensified Reticon photodiode array, with 1024 pixels per channel. The high QE of a thinned, backside charged CCD, especially after AR coating, makes a solid state upgrade very attractive. The difficulty is with large format of the optical system, which is designed for a 40mm image tube. For this reason a CCD mosaic is an excellent canidate as the upgraded detector.

The blue channel has been designed for use with a two-dimensional detector since its inception. An echellette mode is available by placing a 45-degree prism in the beam after dispersion from an echellete grating. This mode has so far only been used with single order blocking filters, a very inefficient observing technique. Short-slit (12 arc sec) spectroscopy is also possible in the cross dispersed mode to obtain spatial resolution with the high spectral resolution of the echellette mode (30 km/sec). Long-slit (2 arc min) spectroscopy can also be achieved with a two-dimensional detector. At the present time, no spatially resolved spectroscopy is possible at the MMT with any instrument. An efficient long-slit mode would therefore be one of the primary goals of the the mosaic detector package.

Detector Considerations

The fast beam of the blue channel Schmidt camera (f/1.6) requires a detector which is very flat. Acid thinned CCDs such as the TI devices are therefore unsuitable as detectors due to their warped imaging surface. The devices produced with chem/mech thinning, however, are flat to $\pm 0.5\mu$m and are very suitable for this application. The optics of the blue channel were optimized for the wavelength range of 3200Å to 5500Å. Tests have been

run which show excellent performance out to the near IR. The wide spatial coverage of CCDs is therefore very advantagous. AR coated thinned CCDs will show greatly reduced fringing in the red, and the stable mounting against a transparent substrate will allow residual fringes to be removed during data reduction.

There are three drawbacks of a CCD mosaic detector when compared to the intensified photon counting system presently used. First, the photon counter has essential no read noise while quality CCDs have a read noise of about 5 electrons. The higher QE of the CCDs (and lower dark current of modern devices) will make up for this effect in most observations. Second, the photon counting system is able to centroid events to less than a physical pixel and thus has higher spatial resolution than a CCD. A 1 arc sec slit is imaged to about 50μm FWHM at the detector image plane without the image stacker, and with it to about 35μm. The Reticon arrays have 4096 effective pixels, each 6μm wide. The FWHM of one resolution element is therefore considerably oversampled. An unintesified CCD cannot be centroided, and has approximatly 500 pixels per device. The 40mm format of the camera requires three CCDs (each about 12mm in physical size), yielding only 1500 pixels. Depending on the CCD used, each pixel is approximately 25μm wide, so a resolution element FWHM is 2 pixels. This is a good match when used with a normal slit or aperture, but undersamples when used with the image stacker.

In the following discussion a specific CCD must be choosen in order to estimate the performance of a blue channel mosaic. While the exact spectral coverage and resolution will depend on which CCD is choosen, I will assume the use of EEV 535x385 22μm pixel devices since they have already been thinned

successfully. Other devices from Thompson, Ford, Reticon, or Tektronix may be the more logical choices depending on their availability and electrical characteristics. Only the details of the design will be changed by using different CCDs, the general performance and overall concepts remain the same. If buttable CCDs are available, and can be thinned and optimzed for blue QE, more significant performance changes (for the better) can be expected. The total length of three EEV sensors mounted as close as possible is approximately 39μm, almost exactly the length of the Reticon arrays.

The physical format of a three CCD mosaic for the blue channel will affect the observing modes in which the spectrograph is used. At the present time, the most common mode uses dual apertures to obtain simultaneous object and sky spectra from 3200Åto 7400Å, with some order overlap redward of 6400Å. The resolution in this mode is about 1Å. The echellette grating is also used with order blocking filters to detect one order at a time, yielding a resolution of 0.5Å. Neither long-slit or cross-dispersed spectroscopy are possible with the present 1-D detectors. Using a three CCD mosaic, these same modes will be available as well as long-slit and cross dispersed spectroscopy.

Long-slit spectroscopy using the present 832 l/mm grating in second order will give a spectral coverage of 932Å at 23.9Å/mm. The two gaps between the CCDs are each 90 pixels wide (2 mm) and amount to a loss of about 48Å. The 400 l/mm grating used in 2nd order gives 1940Å coverage at 49.7Å/mm, with gaps of 99Å. These gaps amount to only 5% of the spectra, which seems quite acceptable. Long-slit spectroscopy is therefore very feasible with a three device mosaic.

The dual aperture mode is also possible with the mosaic detector, with about the same performance as for the long-slit spectroscopy above. The advantage comes with the use of the image stacker, which allows 2.5" apertures to give slightly better resolution than 1" apertures through the use of small optics. The CCD controller used must be capable of binning the six spectra produced into single pixels to avoid excessive read noise penalty. This should present no problem with modern programmable controllers.

Cross dispersed spectroscopy with the mosaic must be done using a short slit to obtain sky spectra due to the limited width of the CCDs. In order to fully separate the spectra of two apertures, a detector width of about 17mm is required. The EEV CCDs are only 8.4mm wide. Simultaneous exposures of object and sky can be obtained using a short slit, with a maximum allowable length of 12 arc seconds. This is certainly a feasible observing method and allows 0.5Å resolution and wide spectra coverage. Some reduction in spectral coverage over what would be possible with a larger format detector must be expected depending on how the orders can be aligned on the CCD. Cross dispersed echellette mode is, however, a very powerful observing technique which can benefit substantially with the use of a CCD mosaic. The wide spectral sensitivity of the CCD is especially well suited for this mode.

Serveral other modifications must be made to the blue channel spectrograph in order to take advantage of a CCD mosaic. These include a new folding flat in the Schmidt camera to allow for the large detector area and possibly modification of the cross dispered prism mount to allow easy change to and from cross dispersed mode. Adequate computer support is needed to reduce the large amount of data to be generated, and a sophisticated CCD

controller must be built to operate the three CCDs. The MMT Blue Channel Spectrograph CCD mosaic will allow not only a first opportunity to problems such as these, but can provide a great improvement in the quality of data obtained with one of the world's largest telescopes on a relatively short time scale.

APPENDIX A

CHEMICAL/MECHANICAL THINNING TECHNIQUE

This appendix explains the chemical/mechanical technique used to thin a silicon CCD from its diced thickness ($\approx 600\mu$m) to 20μm or less, depending on the device type.

I. Preparation for lapping

A. Ready device and outriggers

1. Cut two silicon sample pieces ("outriggers") exactly the same size as the device. These pieces should be diamond sawed, not scribed to avoid edge breaking and lap contamination.
2. Clean outriggers and device in TCE or acetone by soaking them for a few minutes and then wiping with cotton tipped applicators.
3. Cut and clean three 1"x1" microscope slide pieces to be used for an intermediate mount between the silicon and glass disk.

B. Mount silicon on support substrate (glass disk)

1. Clean disk in TCE and heat on hot plate to slightly hotter than mounting wax melting point.

2. Apply wax in pools where silicon is to be mounted. Mounting locations should be halfway between center and disk edge. Use a jig for accurate alignment.
3. Place microscope slide pieces in positions in the wax. With a cotton tipped applicator, gently press pieces to glass to remove air bubbles from wax underneath.
4. Place silicon in proper positions (device frontside down) in the wax. With a cotton tipped applicator, gently press pieces to glass to remove air bubbles from wax underneath.
5. Remove disk from hotplate. Place thin polyurathane sheet over silicon and place five pounds of flat weight on it. Allow wax to fully set.

C. Clean support substrate

1. Remove weights and peel back polyurathane sheet.
2. With cotton tipped applicators and TCE, remove all traces of wax on glass disk. Especially look at the edges of the silicon pieces. Any wax will gum up the polishing operation and thinning will not work. Some wax is allowable during lapping, if removed before polishing begins.

D. Measure silicon height

1. Clean the top of all silicon pieces with a cotton tipped applicator and TCE.

2. Using the dial indicator measure and record the glass disk height. If it is not flat look for contaminates on bottom side.
3. Measure and record the height of all silicon pieces in center and at four corners. If pieces are not flat to $\pm 1\mu$m repeat step B above.

II. Lap silicon

A. Initial thickness to 200μm, thinning rate $\approx$ 10μm per minute

1. Place a conditioning ring on lapping wheel of Lapmaster 12 at a station away from where silicon will be lapped.
2. Place glass disk (silicon side down) on cast iron lapping wheel. Place 1200g of a single centered weight on disk. Place retaining/conditioning ring around disk and weight.
3. Apply 12μm aluminum oxide (Al_2O_3) slurry to wheel and lap five minutes. Be sure silicon is rotaing at all times.
4. Remove disk from wheel, wash slurry and silicon particles off in running water, blow dry. Clean conditioning rings and weights to remove silicon particles.
5. Measure silicon thickness. If outriggers (or device) do not show a tilt is being introduced, determine thinning rate and repeat steps 2—5 (stop at 150μm). If a tilt is found, continue to step 6.
6. Determine which outrigger is thinning slowest. Lay disk back on lap remembering where thickest outrigger is. Load disk off-center so more pressure is applied to thick-

ness outrigger. This will increase the thinning rate on one side to correct for tilt. Continue to step 2.

B. 200μm to 75μm

1. Repeat steps in section A above except use 3μm aluminum oxide slurry instead of 12μm. Stop when silicon is at 75μm. Conditioning ring on unused lapping station is not necessary and may even hinder slurry flow.
2. Clean and dry all Lapmaster parts including weights conditioning rings.

III. Mechanical Polish

A. Clean all surfaces of silicon and glass to remove any trace of Al_2O_3.

B. Using a fairly soft polishing cloth with 0.3μm Al_2O_3 polishing compound, polish silicon for $\approx$ 10 minutes to obtain a specular shine. This improves the chem/mech polishing on some devices.

IV. Chemical/mechanical Polish

A. Prepare silicon

1. As above, clean **every trace** of wax, slurry, and silicon particles from the disk surface and silicon pieces (especially around edges).

B. Prepare polishing lap

1. Mount an unused polishing cloth (PELLON pad) to a flat lapping wheel. Use this wheel only for polishing, never for lapping with slurry.

2. Wash polishing cloth with a stream of water to make sure no particles are embedded in it.

C. Polish silicon

1. Squirt polishing solution in a pool on polishing cloth where disk will be placed. Place disk in pool, silicon side down.
2. Place retaining ring around disk and weight. Note: NEVER use a conditioning ring on the polishing cloth.
3. Turn on polishing machine. Keep polishing solution flowing about ten (10) cc/minute. Never let the cloth dry out.
4. Put 1200g of a single weight on disk. Polish for 20 minutes. Thinning rate is $\approx 1\mu$m/minute.
5. One minute before polishing cycle has ended, stop polishing solution flow and begin flooding cloth with water. This is absolutly necessary to obtain a high quality surface. Continue until polishing machine stops.
6. Remove retaining ring, weight, and disk. Wash all these in running water. Allow disk to try for measurement.
7. Flood polishing cloth again with water to make sure to particles are left on it.
8. Measure height of silicon pieces. Determine thinning rate. Tilt correction may not be possible at this stage. Repeat steps 1— 8 until desired thickness in achieved. On the inintiation of every polishing cycle, look carefully

for any particles (especially wax around silicon edges) and remove them with cotton tipped applicators.

LIST OF REFERENCES

Angel, J.R.P. 1984, "Implementation and Use of Wide Fields in Future Very Large Telescopes", in *Astronomy with Schmidt-Type Telescopes*, Capaccioli, M., ed., Reidel

Béal, G., Boucharlat, G., Chabbal, J., Dupin, J.P., Fort, B., and Mellier, Y. 1987, "Thompson-CSF Frame-transfer Charge-coupled Device Imagers: Design and Evaluation at Very Low Flux Levels", *Opt. Eng.* **26**, 902

Blouke, M.M., Cowens, M.W., Hall, J.E., Westphal, J. A., and Christensen, A. B. 1980, "Ultraviolet Downconverting Phosphor for use with Silicon CCD Imagers", *Appl. Opt.* **19**, 3318

Blouke, M.M., Yang, F.H., Heidtmann, D.L., and Janesick, J.R. 1988, "Traps and Deferred Charge in CCDs", in *Instrumentation for Ground-Based Optical Astronomy: Present and Future*, L.B. Robinson, ed., Springer, Berlin

Blouke, M.M., Janesick, J.R., Hall, J.E., Cowens, W. W., and May, P. J. 1983, "800x800 Charge-coupled Device Image Sensor," *Opt. Eng.* **22**, 607

Bredthauer, R.A., Chandler, C.E., Janesick, J.R., McCurin, T.W., and Sims, G.R. 1988, "Recent CCD Technology Developments" in *Instrumentation for Ground-Based Optical Astronomy: Present and Future*, L.B. Robinson, ed., Springer, Berlin

Burke, B.E., McGonagle, W.H., Mountian, R.W., and Silversmith, D.J. 1980, "A TDI-CCD Hybrid Sensor Mosaic for Satallite Surveillance", *GOMAC*, 77

Cawson, M.G.M., McGraw, J.T., and Keane, M.J. 1986, "The CCD/Transit Instrument (CTI) Data-analysis System", *Proc. SPIE* **627**, 79

Cullum, M., Deiries, S., D'Odorico, S., and Reiss, R. 1985, "Spectroscopy to the Atmospheric Transmission Limit with a Coated GEC CCD", *Astron. Astrophys.* **153**, L1

Driscoll, W.G. 1978, *Handbook of Optics*, p. 7–94, McGraw Hill, New York

Edwards, D.F. 1985, "Silicon", in *Handbook of Optical Constants of Solids*, E.D. Palik, ed., 547–560, Academic Press, Orlando

Ennos, A.E. 1966, "Stresses Developed in Optical Film Coatings," *Appl. Opt.* **5**, 51

Goldmann, L.S., and Totta, P.A. 1983, "Area Array Solder Interconnections for VLSI", *Solid State Technology*, **105**, 91

Gorham, R., Rodger, A., and Stapinski, T. 1982, "STARLAB Detector System: A Wide Field, High Resolution Photon Counting Array", *Proc. SPIE* **331**, 490

Griffiths, R.E., Polucci, G., Mak, A., Murray, S. S., and Schwartz, D. A. 1981, "Single Photon X-ray Imaging with Charge-coupled Devices (CCDs)", *Proc. SPIE* **290**, 62

Gunn, J.E. *et al.* 1987, "Four-Shooter: A Large-Format CCD Camera for the Hale Telescope", Princeton Observatory preprint 212

Gunn, J.E., Harris, F.H., and Oke, J.B. 1987, "The Palomar Observatory CCD Camera", preprint

Heavens, O. 1965, *Physics of Thin Films*, Dover, New York

Hill, J.M. 1987, Columbus Telescope Technical Report

Hlivak, R.J., Henry, J.P., and Pilcher, C.B. 1983, *Proc. SPIE* **445**, 122

Hoffmann, H., and Fischer, G. 1976, "Electrical Conductivity in Thin and Very Thin Platinum Films", *Thin Solid Films*, **36**, 25

Hoffmann, H., Hornamer, H., Jacobs, V., and Vancea, J. 1985, "Electrical Properties of Very Thin Metal Films", *Thin Solid Films*, **131**, 1

Ibrahim, A.A., Yu, K.Y., Gallant, D., White, J.J., Bradley, W.C., Colvin, D.W., and Sandafi, G.J. 1978, "A High Resolution Buttable Time Delay and Integrate Imaging CCD", *Proc. 1978 Int. Conf. Appl. of CCDs*, 1

Janesick, J.R. 1987, JPL Internal Memorandum

Janesick, J., Elliott, T., Collins, S., Marsh, H., Blouke, M., and Freeman, J. 1984, "The Future Scientific CCD", *Proc. SPIE* **501**, 1

Janesick, J., Elliott, T., Daud, T., and McCarthy, J. 1985, "Backside Charging of the CCD", *Proc. SPIE* **570**, 46

Janesick, J., Elliott, T., Daud, T., and Campbell, D. 1986a, "The CCD Flash Gate", *Proc. SPIE* **627**, 543

Janesick, J., Campbell, D., Elliot, T., Daud, T., and Ottley, P. 1986b, "Flash Technology for CCD Imaging in the UV", *Proc. SPIE* **687**, 36

Leach, R. 1987, "Optimizing CCD Detector Operation for Optical Astronomy", *Opt. Eng.* **26**, 1061

Leach, R.W. and Lesser, M.P. 1987, "Increasing the Blue and UV Response of Silicon CCDs", *Publ. Ast. Soc. Pac.* **99**, 668

Lesser M.P. 1987, "Antireflection Coatings for Silicon CCDs", *Opt. Eng.* **26**, 911

Lesser, M.P., Leach, R.W., and Angel, J.R.P. 1986, "Thinning and Mounting a Texas Instruments 3-phase CCD", *Proc. SPIE* **627**, 517

Lind, M.A. and Zalewski, E.F. 1976, *Appl. Opt.* **15**, 1377

Lockhart, R.F. 1982, "Wide Field Planetary Camera for Space Telescope", *Proc. SPIE* **331**, 146

Luppino, G.A., Ceglio, N.M., Doty, J.P., Ricker, G. R., and Vallerga, J. V. 1987, "Imaging and Nondispersive Spectroscopy of Soft X-rays Using a Laboratory X-ray Charge-coupled Device System", *Opt. Eng.* **26**, 1048

Malitson, I.H., 1962, "Refraction and Dispersion of Synthetic Sapphire," *J. Opt. Soc. Am.* **52**, 1377

MacKay, C.D. 1982, "Drift Scan Observations with a Charge-coupled Device", *Proc. SPIE* **331**, 146

Marcus, S., Nelson, R., and Lynds, R. 1979, "Preliminary Evaluation of a Fairchild CCD-211 and a New Camera Design", *Proc. SPIE* **72**, 207

McGraw, J.T., Cawson, M.G.M., and Keane, M.J. 1986, "Operation of the CCD/Transit Instrument (CTI)", *Proc. SPIE* **627**, 60

Mendel, E., and Yang, K. 1969,"Polishing of Silicon by the Cupric Ion Process", *Proc. IEEE*, **57**, 1476

Mizuhashi, M. 1980, "Electrical Properties of Vacuum Deposited Indium Oxide and Indium Tin Oxide Films", *Thin Solid Films*, **70**, 91

Monet, D. 1987, private communication

Morrison, S.R. 1977, *The Chemical Physics of Surfaces*, (New York: Plenum)

Nicollian, E.H. and Brews, J.R. 1982, *MOS (Metal Oxide Semiconductor) Physics and Technology*, (New York: Wiley)

Philipp, H.R., "Silicon Monoxide (Noncrystalline)," in *Handbook of Optical Constants of Solids*, E.D. Palik, ed., 565–569, Academic Press, Orlando

Regh, J. and Silvey, G.A. 1968, "Silicon Planar Chemical Polishing", *Electrochem. Tech.* **6**, 155

Robinson, L. and Osborne, J. 1986, "CCDs at Lick Observatory", *Proc. SPIE* **627**, 492

Smith, D. and Baumeister, P. 1979, "Refractive index of some oxide and fluoride coating materials," *Appl. Opt.* **18**, 111

Stern, R.A. *et al.* 1987, "Ultraviolet and Extreme Ultraviolet Response of Charge-coupled Device Detectors", *Opt. Eng.* **26**, 875

Thorne, D.J., Jorden, P., Waltham, N.R., and van Breda, I.G. 1986, "Laboratory and Astronomical Comparisons of RCA, GEC and Thomson CCDs", *Proc. SPIE* **627**, 530

Tyson, J.A. 1986, "Low-light-level Charge-coupled Device Imaging in Astronomy", *J. Opt. Soc. Am. A* **3**, 2131

Vossen, J.L. 1977, "Thin Metallic Oxides as Transparent Conductors", *Phys. Thin Films*, **9**, 1

Williams, J.T., and Weistrop, D. 1983, "MOSAIC", *Proc. SPIE* **445**, 204